



## Research papers

## Dissolved carbon and CDOM in lake ice and underlying waters along a salinity gradient in shallow lakes of Northeast China

Kaishan Song<sup>a,\*</sup>, Zhidan Wen<sup>a</sup>, Pierre-André Jacinthe<sup>b</sup>, Ying Zhao<sup>a</sup>, Jia Du<sup>a</sup><sup>a</sup> Northeast Institute of Geography and Agroecology, Chinese Academy of Sciences, Changchun, Jilin 130102, China<sup>b</sup> Department of Earth Sciences, Indiana University-Purdue University Indianapolis, IN 46202, USA

## ARTICLE INFO

This manuscript was handled by Huaming Guo,  
Editor-in-Chief

## Keywords:

Closed lakes  
Dissolved carbon  
Open lakes  
Specific conductivity

## ABSTRACT

The variations of DOC and DIC concentrations in lake ice and underlying waters were examined in 40 shallow lakes across the Songnen Plain, Northeast China. The lakes, frozen annually during winter, included freshwater and brackish systems ( $EC > 1000 \mu\text{S cm}^{-1}$ ; range:  $171\text{--}12607 \mu\text{S cm}^{-1}$  in underlying water). Results showed that lake ice contained lower DOC ( $7.2 \text{ mg L}^{-1}$ ) and DIC ( $6.7 \text{ mg L}^{-1}$ ) concentration compared to the underlying waters ( $58.2$  and  $142.4 \text{ mg L}^{-1}$ , respectively). Large differences in DOC and DIC concentrations of underlying waters were also observed between freshwater (mean  $\pm$  SD:  $22.3 \pm 11.5 \text{ mg L}^{-1}$ ,  $50.7 \pm 20.6 \text{ mg L}^{-1}$ ) and brackish lakes ( $83.3 \pm 138.0 \text{ mg L}^{-1}$ ,  $247.0 \pm 410.5 \text{ mg L}^{-1}$ ). A mass balance model was developed to describe the relative distribution of solutes and chemical attributes between ice and the underlying waters. Results showed that water depth and ice thickness were the key factors regulating the spatial distribution of solutes in the frozen lakes. Chromophoric dissolved organic matter (CDOM) absorption coefficient at 320 nm,  $a_{\text{CDOM}}(320)$  and specific UV absorbance ( $\text{SUVA}_{254}$ ) were used to characterize CDOM composition and quality. Compared to the underlying waters, CDOM present in ice largely included low aromaticity organic substances, an outcome perhaps facilitated by ice formation and photo-degradation. In ice and underlying freshwaters, CDOM predominantly included organic C fractions of high aromaticity, while low aromaticity organic substances were observed for brackish lakes. Results of this study suggest that, if water salinity increases due to climate change and anthropogenic activities, significant changes can occur in the dissolved carbon and fate of CDOM in these shallow lakes.

## 1. Introduction

Compared to lakes in tropical or subtropical regions, inland waters (e.g., rivers, lakes, reservoirs) in middle and high latitude from the northern hemisphere contain higher concentrations of dissolved organic carbon (DOC) (Sobek et al., 2007; Spencer et al., 2008; Zhao et al., 2017), which could have a disproportional effect on the global carbon cycle (Cole et al., 2007; Tranvik et al., 2009). DOC acts as a source of energy for heterotrophic bacteria, and the mineralization of allochthonous DOC generally results in a net input of  $\text{CO}_2$  into the atmosphere (Tranvik et al., 2009; Zhang et al., 2010). DOC, the carbon component of dissolved organic matter (DOM), is the pool of organic constituents of water that have neutral buoyancy and pass through a filter with pore size usually ranging from  $0.1$  to  $0.7 \mu\text{m}$  (Mostofa et al., 2009). DOM originates from allochthonous sources (imported from surrounding catchments) and autochthonous sources (produced from phytoplankton or macrophytes in the water body) (Jaffé et al., 2008).

The chromophoric fraction of DOM (CDOM) regulates light transmittance in the water column through absorption of ultraviolet (UV) and photosynthetically active radiation (PAR). In recent years, many studies have been devoted to investigating DOM in sea ice and underlying waters (Belzile et al., 2000; Thomas et al., 2001; Stedmon et al., 2007; Uusikivi et al., 2010; Norman et al., 2011; Müller et al., 2013). Interestingly, Müller et al. (2011, 2013) found that DOM is incorporated to sea ice relatively more than inorganic solutes in the initial ice formation stage, and pointed out that the chemical composition of DOM impacts on enrichment factor. However, very few studies have investigated DOC and CDOM characteristics in lake ice (Belzile et al., 2001, 2002; Song et al., 2017). In frozen lakes, Belzile et al. (2002) reported much lower concentration of DOC and CDOM in the overlying ice than in the underlying waters, a distribution that can affect the light attenuation coefficient of the ice layer for ultraviolet radiation (Mullen and Warren, 1988; Belzile et al., 2001).

Dissolved inorganic carbon (DIC), consisting mainly of dissolved

\* Corresponding author.

E-mail address: [songks@iga.ac.cn](mailto:songks@iga.ac.cn) (K. Song).<https://doi.org/10.1016/j.jhydrol.2019.02.012>

Received 16 May 2018; Received in revised form 18 January 2019; Accepted 1 February 2019

Available online 15 February 2019

0022-1694/ © 2019 Elsevier B.V. All rights reserved.

CO<sub>2</sub>, carbonate and bicarbonate, is the major carbon source for photosynthesis (Wetzel, 2001; Duarte et al., 2008). DIC can be imported to aquatic systems (Wetzel, 2001; Cole et al., 2007; Tranvik et al., 2009; Pacheco et al., 2013; Weyhenmeyer et al., 2015), generated by respiration (Wetzel, 2001) or photochemical or biochemical degradation of DOC and particulate organic carbon (Wetzel, 2001; Weyhenmeyer et al., 2015). Although saline or brackish lakes account for only 20% of the total lake surface area in the world, their water volume is almost equivalent to that of freshwater lakes (Wetzel, 2001; Duarte et al., 2008). Endorheic saline lakes generally exhibit high concentration of dissolved carbon, nutrients and salt due to evaporation (Curtis and Adams, 1995; Brooks and Lemon, 2007; Duarte et al., 2008). Few studies have investigated the characteristics and spatial distribution (in overlying ice and underlying waters) of DOC, CDOM and DIC during the ice formation process in inland water bodies of varying salinity (Belzile et al., 2002; Rysgaard et al., 2007), while it was found that the parent water DOC and CDOM are the dominant factor for determining the counterparts in ice. This finding was also proven by natural sea ice and experimental sea ice studies (Müller et al., 2011, 2013; Xie et al., 2014; Piiparinen et al., 2015). However, the difference of solutes in ice and underlying waters from brackish and fresh water is not clear, and how does it relate to natural ice formation process in the field also needs further investigation.

In lake (or other inland waters) ice, CDOM is an important factor that regulates the biological activity and the optical properties of ice and underlying waters (Belzile et al., 2001, 2002). In the northern hemisphere, lakes can be ice-covered for several months, and available data suggest that the duration of the ice-cover period has shortened due to climate change (Magnuson et al., 2000; Hampton et al., 2008). This could alter light penetration through the ice layer and underlying waters, ultimately affecting biological activity in the water column (Mundy et al., 2007; Hampton et al., 2017). However, there is a paucity of data regarding the properties of dissolved carbon in lake ice and underlying waters (Belzile et al., 2001, 2002; Salonen et al., 2010), particularly in semi-arid regions where saline waters are prevailing. Limited data have shown that lake ice generally contains lower DOC than the underlying water, suggesting an exclusion of DOC during ice formation (Belzile et al., 2001, 2002; Song et al., 2017). The extent of exclusion varies with the chemical species as determined the hydrated radius, diffusivity and solubility of ions through the ice crystal (Pomeroy et al., 2005; Lilbæk and Pomeroy, 2008). At the field-scale, the process can additionally be controlled by the rate of ice formation, and lake water composition at the time of ice crystal initiation. At the present, it is unclear whether this exclusion effect can be observed with DIC and other dissolved solutes in lake waters. Additionally, the optical properties of CDOM in lake ice remain an under-researched area for inland waters, especially significant differences of CDOM between brackish and fresh waters were observed (Song et al., 2017), which may cause light absorption variation for ice and underlying water.

The source and composition of CDOM can be analyzed by fluorescence and UV–visible spectroscopy (Spencer et al., 2008; Helms et al., 2008; Zhao et al., 2017). An investigation by Weishaar et al. (2003) indicated that the specific ultraviolet absorbance (SUVA<sub>254</sub>) is a good tracer to characterize the aromaticity of humic substances in CDOM, and the reactivity of DOC in waters. Several subsequent studies have demonstrated the effectiveness of SUVA<sub>254</sub> as an analytical tool for rapid characterization of CDOM chemistry (Helms et al., 2008; Zhang et al., 2010; Spencer et al., 2012; Song et al., 2017, and references therein). During the formation of lake ice, complex and higher molecular weight molecules of CDOM are generally preferentially expelled into the underlying water, while lower molecular weight molecules are retained within the overlying ice (Belzile et al., 2002; Müller et al., 2013); thus, SUVA<sub>254</sub> might be a useful tracer to examine the chemical differences of CDOM isolated from these two layers.

In this study, DOC, DIC and CDOM within lake ice and underlying waters in lakes across the Songnen Plain, Northeast China, were

examined to determine their optical and chemical characteristics in relation to salinity gradients in these shallow waters. Located in a semi-humid/semi-arid region, waters from the Songnen Plain lakes exhibit a wide range of salinity – from freshwater to brackish lakes. An investigation by Song et al. (2013) has shown that DOC and DIC concentrations in brackish waters were about 3 times higher than in fresh waters across the semi-humid/semi-arid plain of China. However, our knowledge is limited regarding the significance of the exclusion process on the distribution of several dissolved solutes (total dissolved nitrogen (TDN), total dissolved phosphorus (TDP)), algal biomass (using chlorophyll-a as proxy) and total suspended matter (TSM) during ice formation in lakes, particularly shallow waters with high dissolved carbon concentration and salinity. The objectives of this study are to: (1) examine the concentrations of DOC and DIC in lake ice and underlying waters across a wide range of lakes of varying physical, chemical and biological conditions, (2) compare the relative exclusion factor (water/ice ratio) for DOC, DIC, and CDOM in fresh and brackish shallow lakes across the Songnen Plain, and (3) characterize CDOM optical properties, and examine relationships between the concentration of DOC and DIC with salinity in overlying ice and underlying waters.

## 2. Materials and methods

### 2.1. Study sites

The lakes investigated in this study are located in Northeast China (42°49′–49°12′N; 121°38′–128°30′E), and distributed across the Songnen Plain, which is composed of alluvial and lacustrine deposits along the Songhua River and its tributaries (Fig. 1). The region is characterized by many closed-basin lakes, ephemeral lakes and rivers without outlets, resulting in a wide range of freshwater and brackish water bodies (see Fig. S1). The Songnen Plain has a semi-humid to semi-arid monsoon climate. Air temperature decreases from south to north with the annual average temperature ranging from between 2 and 6 °C. The annual average precipitation ranges from 350 to 700 mm with significant inter- and intra-annual variations. About 80% of the annual precipitation occurs between May and September. Surface water bodies are generally covered with ice for more than 4 months each year, typically from November to March.

For this study, 40 water bodies across the Songnen Plain were selected (Fig. 1). Sites were selected according to their size, water depth, outflow conditions and accessibility (Table 1). On the basis of outflow conditions and water electrical conductivity (EC), the lakes were divided into two broad categories: open-water lakes (generally freshwater) and closed water lakes with no outflow (generally brackish water). Fifteen lakes were included in the second category, of which eight are partially connected to a river channel during wet seasons starting from June to September. All the other lakes are connected to the network of streams within the Songhua River watershed (Table 1).

### 2.2. Field sampling and laboratory analysis

Both ice samples and samples from water below the ice were collected during four field campaigns: 14–22 February of 2012, 13–23 February of 2013, 11–18 January of 2014, and 21–31 January of 2015. To further examine the seasonality for water chemical properties and DOC characteristics, field surveys were also conducted in spring 2012 and 2015, and autumn of 2011, 2014 and 2015. For ice-free season sampling, water samples were collected approximately 0.5 m below the water surface, and generally at 3–9 sampling points across each body of water. During winter sampling, water samples were collected at 2 (small lakes) to 5 sampling points (large lakes) across each water body. For the field campaigns conducted during 2011–2014, an ice auger was used to collect ice and underlying water samples. The auger was first drilled into the ice for about 30 cm, and the surface material discarded. The auger was then drilled into the ice for another 30 cm, and all the ice

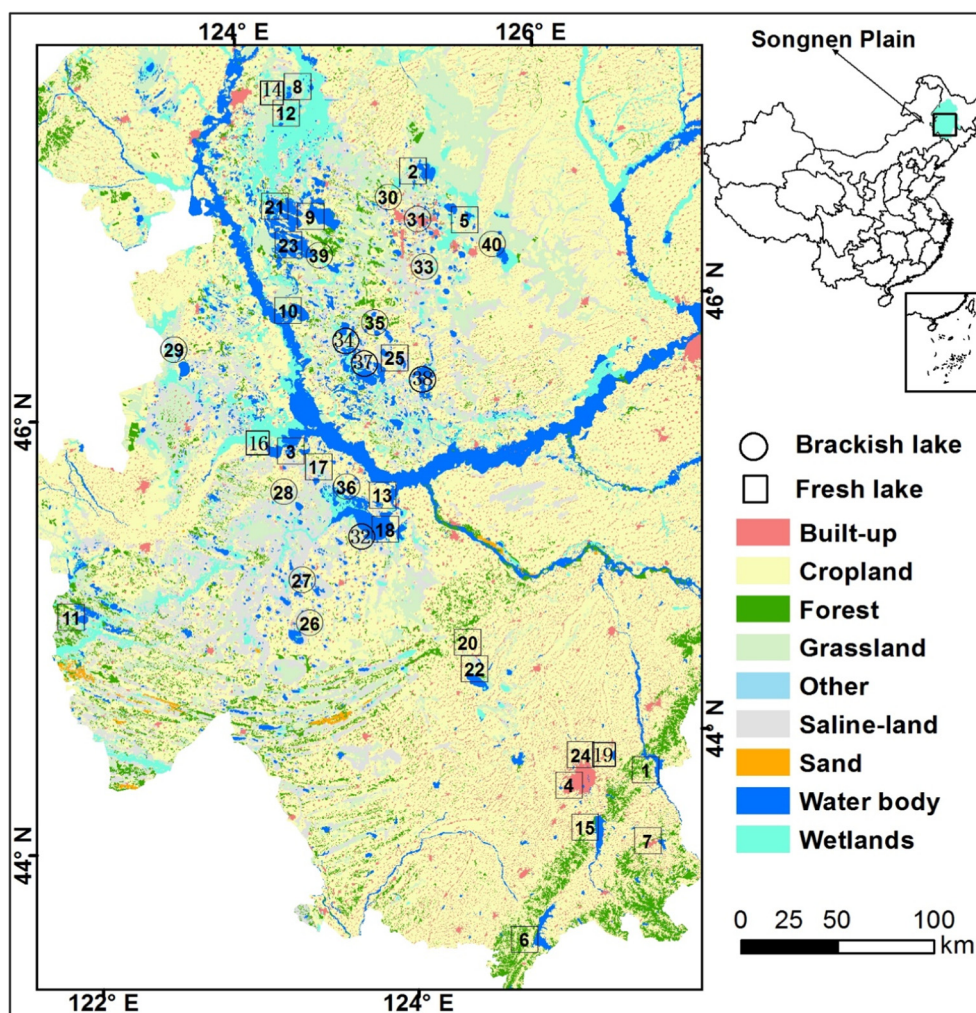


**Fig. 1.** Map of sampling locations across the Songnen Plain, Northeast China. A full description of site names is provided in Table 1. Study sites, numbered 1–25 (inside a square) are freshwater lakes, and sites numbered 26–40 (inside a circle) are brackish lakes. The filled blue area represents the Songnen Plain in China, and the square represents the sampling area within the Songnen Plain. (For interpretation of the references to colour in this figure legend, the reader is referred to the web version of this article.)

shavings drilled from that second layer (30–60 cm) were collected and stored in zip lock bags (see Fig. S2). Finally, the auger was drilled through the entire ice sheet to access the underlying waters. A 2.5-liter plastic water sampler (PWS, Hydro-Bios, Germany) was used to collect water samples just beneath the lake ice. Ice thickness and underlying water depth were recorded. For the 2015 field campaigns, ice cores were collected from the surface (2–27 cm), middle (27–52 cm) and bottom (52–77 cm) layers using a MARK II corer (see Fig. S2; Kovacs Enterprise) and following the method proposed by Belzile et al. (2002).

In addition, four field campaigns were conducted over five lakes distributed in Changchun City and its suburban area to investigate the impact of the ice thickness variation on DOC concentration in underlying waters. The five lakes included Yilan Lake (YLL), Dasui Lake (DSL), Yanming Lake (YML), Nanhu Lake (NHL), and Beihu Lake (BHL), respectively. NHL, YLL, and DSL are located in Changchun City; BHL and YML are located in the suburban area of Changchun City. Due to the easy accessibility, four field campaigns over these five lakes were conducted on 30 October (before ice-on), 29 November, 30 December 2016, and 14 February 2017. The sampling method was similar to that applied in field campaigns conducted in 2015 with MARK II corer.

Ice and underlying water samples were transported to the laboratory for analysis. Ice samples were melted at about 4 °C in the dark, and the melt water was immediately sub-sampled for analysis. Lake water pH and EC ( $\mu\text{S cm}^{-1}$ ) were measured in the laboratory at room

temperature about 21 °C using a pH-meter (PHS-3C; Rex Instrument, Shanghai, China) and conductivity meter (DDS-307 m), respectively. In the laboratory, chlorophyll-a (Chl-a) concentration was determined using a Shimadzu UV-2600 PC spectrophotometer, and TSM was determined gravimetrically as described in Song et al. (2013). DOC and DIC measurements were performed using a high-temperature (680 °C) catalytic oxidation procedure on total organic carbon analyzer (TOC-VCPN, Shimadzu Inc., Japan). Since the analyzer was calibrated to measure DOC in the range of 0–100  $\text{mg C L}^{-1}$ , samples with DOC concentration exceeding 100  $\text{mg C L}^{-1}$  were diluted with Milli-Q water and re-analyzed. These samples were similarly diluted for CDOM absorbance determination to avoid light absorption saturation. Water samples were filtered through pre-combusted 0.45  $\mu\text{m}$  mixed fiber Millipore filters (Bandao Industrial Co., Ltd, China), and the filtrate was analyzed for total dissolved nitrogen (TDN) and total dissolved phosphorus (TDP) concentrations on a Continuous Flow Analyzer (SKALAR, San Plus System, Netherlands; Gross and Boyd, 1998).

### 2.3. CDOM measurements

In the laboratory, water samples were filtered at a low pressure by passing through a pre-combusted Whatman (GF/F) filter (0.7  $\mu\text{m}$ ) and then through a pre-rinsed Millipore filter (0.22  $\mu\text{m}$  pore size). Absorption spectra of the filtrates were obtained between 200 and

**Table 1**

Full name, abbreviated name, and morphological characteristics of the study sites across the Songnen Plain, Northeast China. The spatial distribution of sites (identified by the site number: 1–40) is shown in Fig. 1. N represents the number of samples collected at each site. Abbreviations: volume (V), water depth (D), inflow (In-F) and outflow (Out-F) conditions. Note: R, P, C and G in the In-F column denote river, precipitation, channel and ground water, respectively; Y, N and P in the Out-F column denote outflow, no-outflow, and partial-outflow, respectively.

Site number	Site name	Abbr.	N	A(km <sup>2</sup> )	V (10 <sup>8</sup> m <sup>3</sup> )	D (m)	In-F	Out-F
1	Shitoukou Reservoir	STKR	7	73.3	3.86	7.5	R + P	Y
2	Daqing Reservoir	DQSK	4	56.1	1.03	2.3	C + P	Y
3	Yueliang Lake	YLL	7	206.1	4.75	3.7	R + P	Y
4	Nanhu Lake	NHL	7	1.0	0.03	3.7	SW + R	Y
5	Hongqi Reservoir	HQR	6	26.2	0.83	2.8	C + P	Y
6	Erlong Lake	ELL	9	49.5	2.76	8.4	R + P	P
7	Shuangyang Reservoir	SYR	5	10.2	0.44	3.8	R + P	Y
8	Dongsheng Reservoir	DSR	7	7.8	0.31	3.2	C + P	Y
9	Longhu Lake	LHP	3	130.8	1.75	2.7	R + P	Y
10	Lamasi Lake	LMS	2	51.0	1.52	3.0	R + P	Y
11	Xianghai Lake	XHL	2	19.2	0.78	2.3	P	Y
12	Zhalong Lake	ZLL	4	3.6	0.21	2.4	R + P	P
13	Dakuli Lake	DKL	3	20.5	1.01	2.1	R + P	Y
14	Keqin Lake	KQL	5	18.2	0.34	3.1	R + P	P
15	Xinlicheng Reservoir	XLCR	9	58.2	3.45	7.6	R + P	Y
16	Xinhuang Lake	XHP	3	9.1	0.37	2.3	R + P	Y
17	Tala Lake	TLH	2	6.4	0.26	2.6	P	Y
18	Xinmiao Lake	XMP	4	37.6	0.69	2.4	C + P	Y
19	North Geo-Agro Lake	NGA	3	0.02	0.001	2.6	G + P	N
20	Sidaogang Reservoir	SDGR	2	0.2	0.007	4.6	R + P	P
21	Talahong Lake	TLHL	5	71.6	1.89	1.8	R + P	Y
22	Changjiang Reservoir	CJR	3	12.1	0.77	3.8	C + P	P
23	Huoshaohei	HSH	3	73.4	1.92	2.5	P	Y
24	Beihu Lake	BHL	2	2.3	0.17	2.7	R + P	Y
25	Nanyin Reservoir	NYR	3	47.1	1.05	2.1	C + P	N
26	Dabusu Lake	DUSL	2	35.2	0.64	1.2	P	P
27	Huaapao	HAP	5	24.3	0.37	1.7	R + P	N
28	Ximipao	XMP	4	12.5	0.14	1.5	P	N
29	Yangsapao	YSP	4	38.2	0.86	2.1	R + P	N
30	Yueliangpao	YLP	2	1.1	0.07	1.5	R + P	N
31	Zhaojiatun	ZJT	3	5.6	0.17	1.3	P	N
32	Chagan Lake	CGL	10	375.2	6.42	2.3	C + P	N
33	Zhongneipao	ZNP	5	13.6	0.55	1.7	C + P	N
34	Xinhua Lake	XHL	3	7.4	0.18	1.45	P	N
35	Dongdahui	DDH	3	16.5	0.25	1.37	P	N
36	Xindianpao	XDP	6	58.6	1.12	1.13	P	N
37	Xidahui	XDH	3	12.5	0.46	1.6	P	N
38	Kulipao	KLP	5	33.7	0.71	2.1	R + P	N
39	Yuebingpao	YBP	2	23.0	0.57	2.5	P	N
40	Qingkenpao	QKP	3	33.1	0.73	1.3	C + P	N

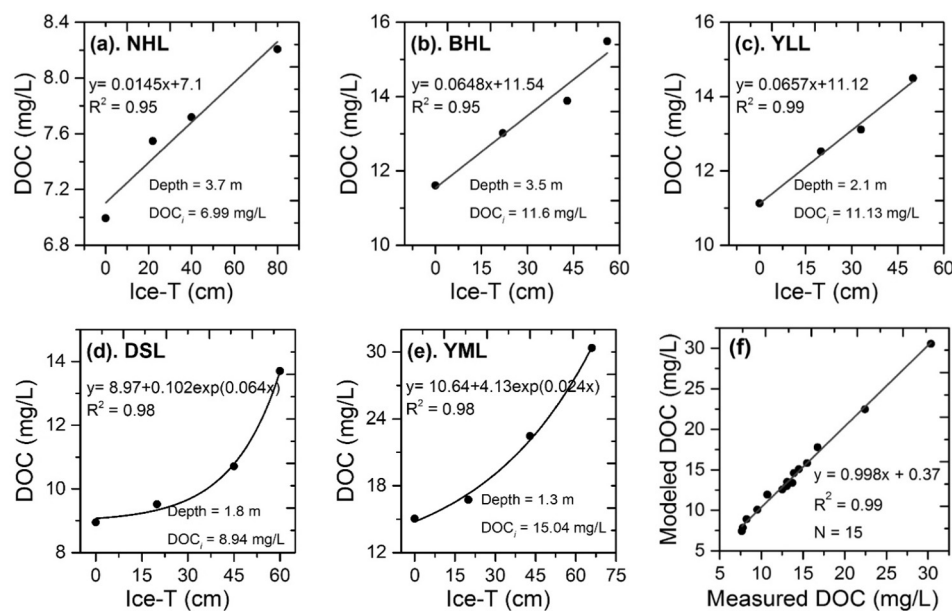


**Fig. 2.** The relationship between DOC concentrations and ice thicknesses in five lakes in Changchun City and around the suburban area. Empirical regression models for (a) Nanhu Lake (NHL), (b) Beihu Lake (BHL), (c) Yilan Lake (YLL), (d) Dasui Lake (DSL), (e) Yanminghu Lake (YML), and (f) relationship between model predicted and measured DOC with pooled data.

**Table 2**

Chemical properties and nutrient concentration in ice and underlying waters in the Songnen Plain lakes investigated. Total dissolved phosphorus (TDP), total dissolved nitrogen (TDN) are reported in mg L<sup>-1</sup>, chlorophyll-a (Chl-a) in µg L<sup>-1</sup>, and specific conductivity (EC) in unit of µS cm<sup>-1</sup>, total suspended matter (TSM) in mg L<sup>-1</sup>, Ice-T, ice thickness (cm). Full names of the study sites are listed in Table 1.

Site Abbr.	Underlying water samples						Ice samples						Ice-T
	pH	TDP	TDN	Chl-a	EC	TSM	pH	TDP	TDN	Chl-a	EC	TSM	
STKR	7.5	0.05	1.3	10.2	278	2.2	7.5	0.03	0.5	1.3	12	1.1	85
DQSK	8.6	0.05	0.8	13.4	170	3.2	7.9	0.03	0.6	0.3	45	2.6	87
YLL	7.7	0.06	1.9	10.1	355	25.9	7.9	0.02	0.4	0.3	9	9.5	103
NHL	7.7	0.08	1.9	11.2	369	3.4	7.4	0.05	0.7	1.3	54	2.5	68
HQR	8.1	0.04	1.1	9.0	257	3.0	7.7	0.02	0.5	0.5	47	1.8	101
ELL	8.2	0.05	1.7	17.3	354	2.3	7.4	0.03	0.5	0.6	12	3.4	73
SYR	7.4	0.05	1.4	2.9	377	1.7	7.0	0.03	0.4	0.4	16	1.2	86
DSR	7.5	0.06	2.0	22.6	322	14.4	7.6	0.05	0.9	0.8	52	8.6	88
LHP	8.0	0.2	1.3	9.3	340	18.9	7.7	0.02	0.7	0.3	45	3.6	87
LMS	8.3	0.1	2.6	9.5	282	17.3	8.7	0.05	0.8	1.1	38	7.3	76
XHL	7.4	0.06	0.7	38.6	330	6.3	8.3	0.02	0.4	1.3	11	2.7	98
ZLL	7.3	0.1	2.6	40.8	312	95.0	8.1	0.03	0.9	1.4	6	18.5	100
DKL	7.8	0.09	1.6	10.9	327	6.5	8.4	0.02	0.6	0.7	16	8.2	95
KQL	8.2	0.05	1.3	22.8	519	11.9	7.5	0.02	0.6	0.5	46	3.7	92
XLCR	7.7	0.08	1.0	8.5	378	1.9	7.6	0.02	0.5	0.5	16	2.6	70
XHP	8.2	0.05	2.0	10.2	291	13.4	6.4	0.02	0.4	0.3	2	7.5	84
TLH	7.9	0.28	1.7	7.2	584	22.3	7.8	0.02	0.4	0.5	15	11.2	96
XMP	7.7	0.08	1.4	15.4	773	1.3	7.9	0.02	0.7	0.4	50	3.9	89
NGA	7.7	0.01	1.8	14.0	496	7.0	7.4	0.01	0.5	0.3	3	3.3	78
SDGR	7.3	0.05	2.1	6.9	510	24.9	8.5	0.04	0.4	1.3	32	17.6	76
TLHL	7.8	0.24	1.5	8.6	735	7.3	7.7	0.08	0.3	0.4	5	1.7	93
CJR	7.6	0.04	2.1	4.3	657	7.9	8.5	0.02	0.7	0.3	55	2.9	68
HSB	8.3	0.06	2.2	3.2	770	3.1	8.2	0.03	1.2	0.2	53	1.2	88
BHL	7.5	0.22	1.5	12.5	935	29.9	7.4	0.10	0.5	0.5	13	11.4	72
NYR	8.4	0.11	7.7	6.6	1306	56.4	8.0	0.05	0.7	0.3	33	9.2	93
DUSL	7.9	0.14	1.8	9.3	1331	2.7	7.8	0.05	0.6	0.6	42	1.4	102
HAP	8.6	0.07	2.2	31.2	1597	2.0	9.0	0.07	0.5	0.3	55	0.8	95
XMP	8.6	0.41	2.1	18.6	1729	4.3	8.5	0.04	0.7	0.9	9	2.1	95
YSP	8.1	0.08	25.7	23.4	1326	146.0	8.2	0.03	1.7	0.3	33	19.5	98
YLP	7.9	2.25	2.5	5.1	1054	19.3	7.8	0.11	0.7	0.6	35	15.2	92
ZJT	7.7	0.22	2.9	8.0	1040	19.6	7.7	0.05	0.4	0.5	29	12.4	88
CGL	8.6	0.07	19.1	10.8	1205	19.3	8.4	0.03	1.0	1.6	175	7.8	115
ZNP	8.3	3.52	3.0	40.2	2048	3.7	8.5	0.25	1.9	2.9	1189	3.7	92
XHL	9.0	0.55	2.3	79.6	2133	228.8	9.8	0.42	1.9	1.3	807	87.2	55
DDH	9.7	3.96	4.6	67.8	3203	15.6	9.9	2.73	0.6	3.6	153	24.1	68
XDP	8.1	0.13	3.5	27.8	3430	327.7	8.9	0.04	1.1	1.9	145	103.7	86
XDH	9.0	4.77	6.9	78.3	3227	60.8	9.6	0.48	1.0	1.7	76	21.4	92
KLP	8.5	1.36	8.0	107.4	3010	31.1	8.8	0.05	5.4	2.9	165	8.9	87
YBP	8.9	0.5	12.4	41.5	4430	197.1	8.5	0.35	1.4	1.6	728	26.4	78
QKP	9.0	2.84	1.3	47.2	12607	77.1	9.8	0.16	0.5	1.3	12	23.0	98

800 nm at 1-nm increment with a Shimadzu UV-2660 PC dual beam spectrophotometer using a 3 cm quartz cuvette. Milli-Q water was used as reference for measuring CDOM absorption. Following the procedure from Babin et al. (2003), the absorption coefficient [ $a_{\text{CDOM}}(\lambda)$ ] was calculated from the measured optical density (OD) via Eq. (1):

$$a_{\text{CDOM}}(\lambda) = 2.303[OD_{S(\lambda)} - OD_{(\text{null})}]/\gamma \quad (1)$$

where  $\gamma$  is the cuvette path length (0.03 m), and OD (null) is the average optical density in the spectral range of 740–750 nm, which is assumed to be zero (Babin et al., 2003). All absorption measurements were made within 48 h after field collection. The SUVA<sub>254</sub> proposed by Weishaar et al. (2003) was used as an indicator of the CDOM aromaticity, which is computed as  $a_{\text{CDOM}}(254)$  divided by the DOC concentration (mg C L<sup>-1</sup>).

#### 2.4. Impact of ice thickness on water chemistry parameters

Exclusion factors for water parameters were determined as the ratio of concentrations in water to the concentration in ice (Belzile et al., 2002). Previous investigations (Belzile et al., 2002; Zhang et al., 2012; Xue et al., 2016) have shown that ice formation in inland waters can have a strong impact on the distribution of solutes within the ice and in the underlying water column, and the same situation was observed for CDOM, DOC with sea ice growing experiments (Müller et al., 2013). As

shown in Fig. 2, variations in water depth ( $D_w$ ), ice thickness ( $I_i$ ) and DOC concentration before ice formation in autumn resulted in different regression models between DOC concentration in the underlying water and ice thickness. As a relatively deep water, the ice thickness exerted less impact on DOC for the NHL (Fig. 2a) by showing smaller regression slope (0.014), while ice thickness exerted a significant impact on DOC concentration for the DSL (Fig. 2d) and YML (Fig. 2e) due to the water depth by showing different regression coefficients. It also can be seen that the regression slope (Fig. 2a–c) increases with the water depth since the ice thicknesses were close for these lakes. Thus, in light of these preliminary findings, we developed a model to predict the concentration of different solutes in the underlying waters using lake morphological attributes and solute concentration ( $S_0$ ) in lake waters before initiation of ice formation. Suppose  $S_i$  is the solute concentration in the ice and assuming mass balance, the following equation can be written:

$$D_w \times S_0 = S_u \times (D_w - I_i) + S_i \times I_i \quad (2)$$

where  $S_u$  is the solute concentration in the underlying water. As may be found out that the exclusion factor is indeed very high in the waters investigated in this study, thus the bulk solute mass in ice can be ignored,  $S_u$  can be derived as:

$$S_u = (D_w \times S_0)/(D_w - I_i) \quad (3)$$

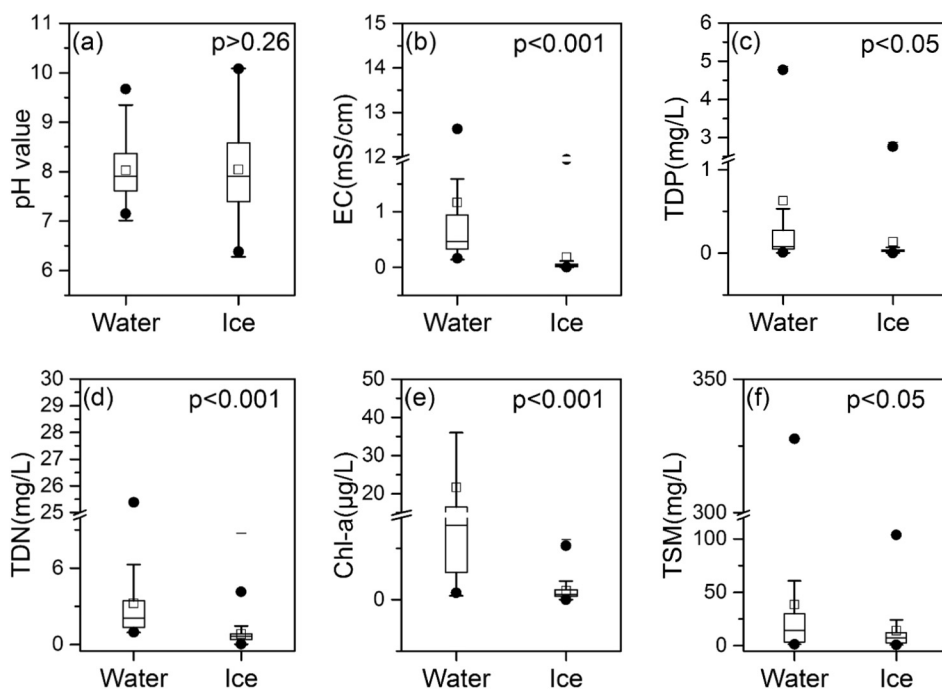


Fig. 3. Boxplot of water quality parameters in ice melted water and underlying water samples. The black line and the open square represent the median and mean respectively. The horizontal edges of the boxes denote the 25th and 75th percentiles; the whiskers denote the 1st and 99th percentiles and the filled circles represent outliers.

As shown in Fig. 2f, the model (Eq.3) performed well, and thus was used to evaluate the impact of  $D_w$ ,  $I_b$  and  $S_o$  on underlying water chemistry at the 40 lakes across the Songnen Plain examined in the present study.

### 2.5. Statistical analyses

Statistical analyses were conducted using MatLab 2009B software package (MathWorks Inc., FL). Differences in bio-physicochemical parameters (pH, EC, DOC, DIC,  $a_{CDOM}(320)$ ,  $SUVA_{254}$ , Chl-a, TSM and exclusion factors, EF) between overlying ice and underlying waters at each study station were assessed using paired *t* test. In addition, analysis of variance (ANOVA) was carried out, separately for ice and underlying waters, to assess differences between brackish and freshwater lakes in the Songnen Plain. Partial least square analysis, correlation analyses, and regression analyses were also conducted (OriginPro2016 software package, Origin Lab Corporation) to examine relationships between lake morphology, water chemical and optical properties.

## 3. Results

### 3.1. General characteristics

The 40 investigated lakes in the Songnen Plain were quite diverse based on limnetic conditions and the physicochemical attributes of lake waters (Tables 1, 2, S1). The thickness of the ice layer ranged between 0.68 and 1.15 m depending on the initial date of each field campaign, air temperature and lake morphology. Based on lake water salinity (as determined by EC values recorded during the ice-free season; Table S2), the Songnen Plain lakes were grouped into freshwater ( $EC < 1000 \mu S cm^{-1}$ ; numbered 1–25) and brackish water systems (numbered 26–40) (Tables 1 and 2). As demonstrated in Table S2, the average EC was  $1999.8 \pm 1056 \mu S cm^{-1}$  in brackish water lakes, which was significantly higher ( $p < 0.001$ ) than that in fresh lakes ( $417.2 \pm 212.1 \mu S cm^{-1}$ ) during the ice free season. In winter, the EC of underlying waters in average was  $2803.4 \pm 2941 \mu S cm^{-1}$  in the brackish lakes, significantly ( $p < 0.001$ ) higher than that in the freshwater lakes ( $534.5 \pm 332 \mu S cm^{-1}$ , Table 2). In the ice free season, the average pH of brackish waters is significantly higher than

that in fresh waters (9.1 vs. 8.2,  $p < 0.005$ ; Table S1). Likewise, the pH of the underlying waters was significantly higher in brackish than that in freshwater lakes (8.6 vs. 7.8,  $p < 0.05$ ) in winter.

This comparison indicates that TDP and TDN exhibited large variability in both ice free and ice on seasons (Table S1, 2). The concentration of TDP (TDN) in ice free season ranged from 0.007 to  $2.1 mg PL^{-1}$  ( $0.4$  to  $11.6 mg NL^{-1}$ ) with an average concentration of  $0.29 \pm 0.45 PL^{-1}$  ( $1.90 \pm 1.91 PL^{-1}$ ) in the ice free season. In ice on season, TDP (TDN) concentration ranged from 0.01 to  $4.77 mg PL^{-1}$  ( $0.7$  to  $25.7 mg NL^{-1}$ ) with a mean of  $0.56 \pm 1.16 mg PL^{-1}$  ( $3.63 \pm 4.98 mg NL^{-1}$ ). High concentrations of Chl-a ( $56.6 \pm 51.2 \mu g L^{-1}$ ) were measured, ranging from 3.7 to  $230.2 \mu g L^{-1}$  in ice free season. In winter, relatively high concentrations of Chl-a ( $28.6 \pm 23.8 \mu g L^{-1}$ ) were recorded in the underlying water samples, indicating that biological processes were still active below the lake ice sheet. A strong correlation of Chl-a between ice free season and ice on season was revealed ( $R = 0.73$ ,  $p < 0.01$ ). The lakes in the Songnen Plain were extremely turbid because of high TSM concentration ( $121.0 \pm 286.7 mg L^{-1}$ ) in ice free season. A much lower averaged TSM ( $38.6 \pm 69.6 mg L^{-1}$ ) was recorded in the water beneath lake ice. According to the trophic state index classification proposed by Carlson (1977), the 40 lakes were either hypereutrophic (25%), eutrophic (55%) or mesotrophic (20%) in winter season, and even worse in ice free season (hypereutrophic: 32%, eutrophic: 63%, and mesotrophic: 5%). We detected a significant relationship between Chl-a concentration in the ice layer and that in the underlying water (Fig. S3b), suggesting that perhaps most of the Chl-a in ice is derived from underlying waters. With regard to Chl-a concentration in underlying water, our analysis suggested a seasonal carry-over effect as illustrated by the relationship ( $R^2 = 0.66$ ) between Chl-a concentration in the previous autumn and that measured during the next winter (Fig. S3a). Partial least square analysis indicated that Chl-a concentration in the underlying waters was correlated positively with TDP, TDN and DOC, and negatively with ice thickness ( $I_b$ ) and snow cover fraction (SCF) [ $Chl-a = 7.2 * TDP + 0.75 * TDN + 0.37 * DOC - 41.75 * I_b - 0.21 * SCF - 0.05 * DIC + 61.1$ ]. These factors explained 48.3% of the variation in the Chl-a concentration measured in the underlying waters, with TDP,  $I_b$  and SCF being the dominant factors.

While the pH values of melted lake ice and the underlying waters

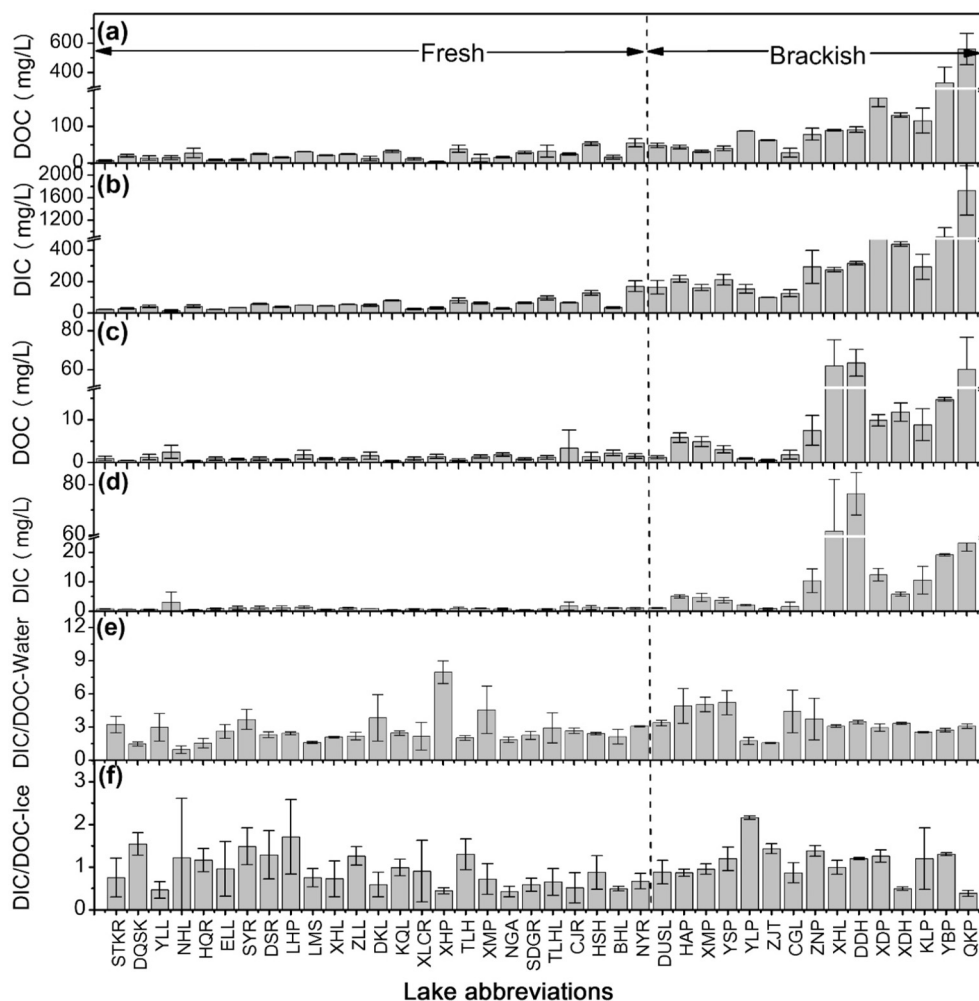


**Fig. 4.** Variation in the concentration of DOC and DIC in ice and underlying waters collected in lakes across the Songnen Plain in winter; (a) DOC and (b) DIC concentrations from fresh and brackish waters, (c) DOC and (d) DIC concentrations from corresponding ice samples, and (e)–(f) DIC/DOC ratios for underlying waters and ice samples, respectively. Full names of the study sites are listed in Table 1.

were generally similar ( $p > 0.26$ ), EC, TDP, TDN, Chl-a and TSM concentrations were much lower in the overlying ice than in the underlying waters (Table 2, Fig. 3). The average EC of melted lake ice ( $238 \mu\text{S cm}^{-1}$ ) was significantly lower ( $p < 0.01$ ) than in the underlying waters ( $1364 \mu\text{S cm}^{-1}$ ). The concentration of Chl-a in lake ice water samples (range:  $0.23\text{--}5.8 \mu\text{g L}^{-1}$ ) was significantly lower ( $p < 0.001$ ) than that detected in the underlying water samples (Fig. 3e and Table 2). Similar trends were observed for TSM (Fig. 3f), TDN and TDP (Fig. 3c and d).

### 3.2. Dissolved carbon concentration

High concentrations of DOC (DIC) were measured in the Songnen Plain lakes (Table S1), and the average concentrations were  $23.7 \pm 26.2 \text{ mg CL}^{-1}$  and  $80.8 \pm 101.0 \text{ mg CL}^{-1}$  for DOC and DIC in ice free season, respectively. Significant differences were observed for DOC ( $p < 0.01$ ) and DIC ( $p < 0.01$ ) concentrations in fresh (DOC:  $12.7 \pm 0.1 \text{ mg CL}^{-1}$ ; DIC:  $36.7 \pm 25.8 \text{ mg CL}^{-1}$ ) and brackish (DOC:  $41.9 \pm 35.9 \text{ mg CL}^{-1}$ ; DIC:  $154.1 \pm 134.4 \text{ mg CL}^{-1}$ ) waters during ice free season. As shown in Table S3, obvious seasonal variations were demonstrated in spring, autumn and winter. Significant difference ( $p < 0.001$ ) was noted between the melted lake ice and underlying waters with respect to DOC and DIC concentrations (Fig. 4, Tables 3 and S3). Averaged across all lakes, DOC concentrations in underlying waters were significantly higher ( $58.2 \text{ mg CL}^{-1}$ ) than in the melted ice

( $7.2 \text{ mg CL}^{-1}$ , Table S3). As demonstrated in Fig. 4b and d, a much higher concentration of DIC was measured in the underlying waters ( $142.4 \text{ mg CL}^{-1}$ ) than in the melted ice ( $6.7 \text{ mg CL}^{-1}$ ), and EF values in Table 3 further demonstrated the difference between melted ice and underlying waters.

Significant differences ( $p < 0.0001$ ) were observed between freshwater (mean/median  $\pm$  SD:  $22.3/20.1 \pm 11.5 \text{ mg CL}^{-1}$ ) and brackish lakes ( $123.5/83.3 \pm 138.0 \text{ mg CL}^{-1}$ ) with regard to DOC concentrations in the underlying waters (Fig. 4a). Similar trends were noted with DIC, with concentrations in brackish waters ( $p < 0.0001$ ;  $382.2/247.0 \pm 410.5 \text{ mg CL}^{-1}$ ) being several-fold higher than that in freshwater lakes ( $50.7/44.5 \pm 20.6 \text{ mg CL}^{-1}$ ). The concentration of DOC in melted lake ice (Fig. 4c) followed a pattern similar to that observed with the underlying waters, meaning DOC concentrations in brackish lakes (mean/median:  $6.2/2.2 \pm 23.1 \text{ mg CL}^{-1}$ ) were significantly higher than those in freshwater lakes ( $1.2/0.9 \pm 1.1 \text{ mg CL}^{-1}$ ). Likewise, DIC concentrations in melted ice samples from brackish lakes ( $15.3/3.7 \pm 23.1 \text{ mg CL}^{-1}$ ) were significantly higher ( $p < 0.001$ ) than in samples from freshwater lakes ( $1.1/0.76 \pm 1.3 \text{ mg CL}^{-1}$ ).

The ratios of DIC/DOC in both underlying waters and melted ice samples were presented in Fig. 4e and f. The average DIC/DOC ratio of underlying water in fresh water lakes was  $2.59 \pm 1.35$ , which was significantly different ( $p < 0.05$ ) from brackish lakes ( $3.41 \pm 1.10$ ). As for ice melted samples, no significant difference ( $p = 0.74$ ) was

**Table 3**

Exclusion factors (underlying water/ice) for total phosphorus (TP), total nitrogen (TN), chlorophyll-a (Chl-a), dissolved inorganic carbon (DIC), dissolved organic carbon (DOC), pH, specific conductivity (EC), and  $a_{\text{CDOM}}(320)$  in lake waters across the Songnen Plain.

Site abbr.	TDP	TDN	Chl-a	DIC	DOC	pH	EC	$a_{\text{CDOM}}(320)$	TSM
STKR	2.3	12.5	13.7	31.8	9.9	1.0	40.7	32.3	1.2
DQSK	1.6	1.4	6.4	40.5	43.2	1.1	4.0	85.1	0.9
YLL	4.8	9.5	37.0	76.9	17.6	1.0	97.6	32.0	1.1
NHL	1.7	6.4	12.8	16.9	7.2	1.0	16.5	25.5	2.3
HQR	1.7	2.1	23.7	95.6	63.9	1.1	6.9	115.9	0.8
ELL	2.	19.6	38.3	29.9	12.9	1.1	40.4	17.8	0.7
SYR	1.8	19.3	7.9	36.5	13.2	1.0	29.7	20.8	1.6
DSR	1.2	2.3	68.2	55.5	30.8	1.0	6.7	35.5	0.5
LHP	8.7	1.8	27.4	40.3	25.5	1.0	6.4	23.3	57.5
LMS	2.5	3.4	10.2	38.3	20.1	0.8	8.7	35.6	0.7
XHL	2.1	1.8	2.7	82.6	54.1	0.8	130.9	16.2	3.4
ZLL	3.3	3.7	655.9	51.7	29.7	0.8	64.8	17.1	0.8
DKL	5.0	3.0	24.3	50.0	9.9	0.9	75.0	50.4	7.4
KQL	2.0	2.5	3.3	182.8	72.0	1.1	8.5	44.0	4.3
XLGR	8.5	3.8	21.0	34.8	22.1	1.0	36.8	22.2	6.1
XHP	8.0	5.0	19.0	149.5	69.6	1.0	326.0	26.0	0.4
TLH	14.0	5.1	19.2	65.2	12.6	1.0	94.8	72.8	1.0
XMP	8.4	2.1	1.6	38.0	8.7	1.1	9.9	4.1	1.3
NGA	0.8	3.4	48.9	133.4	35.1	0.9	171.1	52.1	0.6
SDGR	1.3	10.1	10.8	124.2	33.4	1.0	39.9	54.7	8.1
TLHL	3.7	3.6	6.0	59.5	20.7	0.9	154.3	88.1	1.5
CJR	1.8	3.0	13.0	131.5	46.9	1.0	14.7	56.8	1.6
HSB	1.8	2.2	2.1	31.6	7.2	1.0	14.5	2.8	0.3
BHL	8.8	3.1	24.5	140.3	34.2	1.0	96.3	23.2	0.4
NYR	2.2	10.5	88.3	128.7	120.8	1.0	41.5	127.7	0.8
DUSL	2.9	11.3	87.3	37.3	63.3	1.0	28.3	50.2	0.6
HAP	6.3	2.7	52.3	66.9	27.5	1.1	37.7	81.2	1.4
XMP	2.7	4.6	8.5	28.0	33.7	1.1	16.4	17.5	3.4
YSP	14.7	15.7	7.4	73.7	90.0	1.0	22.3	32.9	10.7
YLP	20.9	3.4	11.0	132.3	29.7	1.1	27.3	42.6	1.5
ZJT	4.4	9.9	16.2	120.5	21.5	1.0	90.9	56.4	1.0
CGL	3.8	18.9	70.5	89.5	41.8	1.0	19.2	88.8	0.3
ZNP	36.4	1.6	41.6	4.9	1.5	0.9	1.9	1.6	0.8
XHL	1.5	1.2	1.7	4.2	1.5	1.0	4.0	1.4	1.9
DDH	1.5	8.4	542.1	434.6	181.2	0.9	991.3	142.0	69.8
XDP	3.3	3.1	61.2	76.0	11.4	0.9	26.4	13.1	2.8
XDH	10.3	7.4	172.8	94.9	48.6	1.0	56.9	124.3	1.7
KLP	32.6	0.9	8.7	47.7	22.8	1.3	26.3	9.1	3.1
YBP	0.3	8.9	141.2	73.7	9.3	0.9	17.2	21.4	2.1
QKP	18.5	12.5	13.7	31.8	9.9	1.0	40.7	32.3	1.3

observed for the DIC/DOC ratio of fresh ( $0.91 \pm 0.38$ ) and brackish ( $1.09 \pm 0.42$ ) water lakes. Further, significant difference was observed for the DIC/DOC ratio between melted ice and underlying waters ( $p < 0.001$ , Fig. 4e versus Fig. 4f); likewise significant differences were observed for the melted ice and underlying waters in fresh water systems ( $p < 0.001$ ), and brackish water systems ( $p < 0.001$ ).

Strong relationships were found between DOC and DIC in both the underlying ( $r^2 = 0.97$ , Fig. 5a) and the melted lake ice waters ( $r^2 = 0.85$ , Fig. 5b). The slopes of the regression lines suggested that DIC concentration was about three times higher than DOC in the underlying water column (Fig. 5c), but DOC and DIC were present in almost equal concentration in the ice sheet (Fig. 5b).

### 3.3. Colored dissolved organic matter

A significant difference ( $p < 0.005$ ) was observed for the absorption coefficient of CDOM at 320 nm [ $a_{\text{CDOM}}(320)$ ] between fresh ( $6.32 \pm 3.01 \text{ m}^{-1}$ ) and brackish ( $23.89 \pm 16.51 \text{ m}^{-1}$ ) waters during the ice free season. In winter, significant differences ( $p < 0.001$ ) were also observed for  $a_{\text{CDOM}}(320)$  of fresh and brackish waters. Across all the study sites,  $a_{\text{CDOM}}(320)$  in average was  $9.42 \pm 4.41 \text{ m}^{-1}$  and  $48.60 \pm 27.34 \text{ m}^{-1}$  in fresh and brackish waters, respectively. The  $a_{\text{CDOM}}(320)$  was lower in the melted lake ice than in the underlying waters (Fig. 6b), with the average  $a_{\text{CDOM}}(320)$  for underlying waters

being about ten times higher than that of melted lake ice waters. Likewise, the averaged  $a_{\text{CDOM}}(320)$  of melted lake ice was  $0.47 \text{ m}^{-1}$  in freshwater lakes, which is significantly ( $p < 0.001$ ) lower than that in brackish lakes ( $3.03 \text{ m}^{-1}$ ).

The averaged  $\text{SUVA}_{254}$  was  $2.30 \text{ L mg C}^{-1} \text{ m}^{-1}$  during ice free season, and demonstrated an obvious spatial variability (range:  $0.34\text{--}8.76 \text{ L mg C}^{-1} \text{ m}^{-1}$ , coefficient of variation, CV%: 56.5%). As shown in Fig. 6c, d, the  $\text{SUVA}_{254}$  values recorded in the freshwater systems exhibited a larger variability (range:  $1.01\text{--}6.10 \text{ L mg C}^{-1} \text{ m}^{-1}$ ; CV: 48.9%) compared to the brackish lakes (range:  $0.76\text{--}3.31 \text{ L mg C}^{-1} \text{ m}^{-1}$ , CV: 36.7%). Further, significant differences ( $p < 0.05$ ) in  $\text{SUVA}_{254}$  were also observed between freshwater (range:  $0.38\text{--}2.86 \text{ L mg C}^{-1} \text{ m}^{-1}$ , CV: 47.6%) and brackish (range:  $0.11\text{--}2.07 \text{ L mg C}^{-1} \text{ m}^{-1}$ , CV: 63.3%) systems in melted ice waters. There was no significant difference ( $p = 0.56$ ) in  $\text{SUVA}_{254}$  between waters during ice free season and that in underlying waters in winter. However, a significant difference ( $p < 0.001$ ) in  $\text{SUVA}_{254}$  was observed between melt ice ( $1.18 \pm 0.64 \text{ L mg C}^{-1} \text{ m}^{-1}$ ) and underlying waters ( $2.16 \pm 1.02 \text{ L mg C}^{-1} \text{ m}^{-1}$ ), where relatively higher  $\text{SUVA}_{254}$  was observed in the underlying waters than in the overlying ice, regardless of lakes salinity (Fig. 6c, d).

### 3.4. Dissolved carbon versus specific conductivity

Regression analysis showed strong relationships ( $R^2 > 0.80$ ;  $p < 0.001$ ) between EC and the concentrations of DOC and DIC (Fig. 7). It is worth noting that the slopes of regression lines (0.043 for DOC in Fig. 7a; 0.14 for DIC in Fig. 7b) were different for underlying waters, but were very close (0.064 for DOC in Fig. 7c; 0.057 for DIC in Fig. 7d) for melted lake ice waters.

### 3.5. Ice thickness impact and exclusion factors

We applied Eq. (3) to calculate the concentrations of solutes and particles in the underlying water based on the measured concentrations in the autumn, and the lake water depth ( $D_w$ ) and ice thickness ( $I_t$ ) (the data was presented in both Tables 1 and S1). The impacts of  $D_w$  and  $I_t$  on different physical and chemical properties of lake waters were evaluated. The model predicted DOC and DIC concentrations very well as shown by the good match with measured concentrations in the underlying waters (Fig. 8a, b). As shown in Fig. 8c, d, the model performed less well for TDP and TDN, and the performance was good for EC (Fig. 8e) and  $a_{\text{CDOM}}(320)$  (Fig. 8f).

The exclusion factors (water/ice) for various constituents in ice-covered lakes in the Songnen Plain varied considerably depending on the chemical element considered (Table 3). No obvious exclusion was observed for pH (Fig. 9a), but the largest variation in exclusion factors was recorded for EC (Fig. 9b; range: 1.4–991.3; mean: 72.2). The exclusion factors were more variable for TDP (Fig. 9c; range: 0.3–36.4; mean: 6.4) than for TDN (Fig. 9d; range: 0.9–21.6; mean: 6.3). Exclusion factors were also larger and more variable for Chl-a (Fig. 9e; range: 1.5–655.9; mean: 59.2) than for TSM (Fig. 9f; range: 0.3–69.8; mean: 5.1). The exclusion factors for DOC (Fig. 9g; range: 1.5–181.2; mean: 35.3) were of similar magnitude to those obtained for  $a_{\text{CDOM}}(320)$  (Fig. 9i; range: 1.4–151.1; mean: 45.4), but were smaller and less variable than the exclusion factors for DIC (Fig. 9h; range: 4.2–434.6; mean: 78.3). Of all the parameters considered (Table 3), TDP was the only chemical constituent for which the exclusion factor was significantly different between fresh water and brackish water systems (Fig. 9c).

The vertical distribution of various chemical and physical elements in the ice sheet was examined (Fig. 10). Except for EC, the distribution of elements in the ice profile was generally similar, with significantly higher concentration ( $p < 0.05$ ) in the upper layer than that in the middle and bottom layers of the ice sheet. As shown in Fig. S5, except pH, the ratios of solutes or particle in upper ice layer (middle layer) to

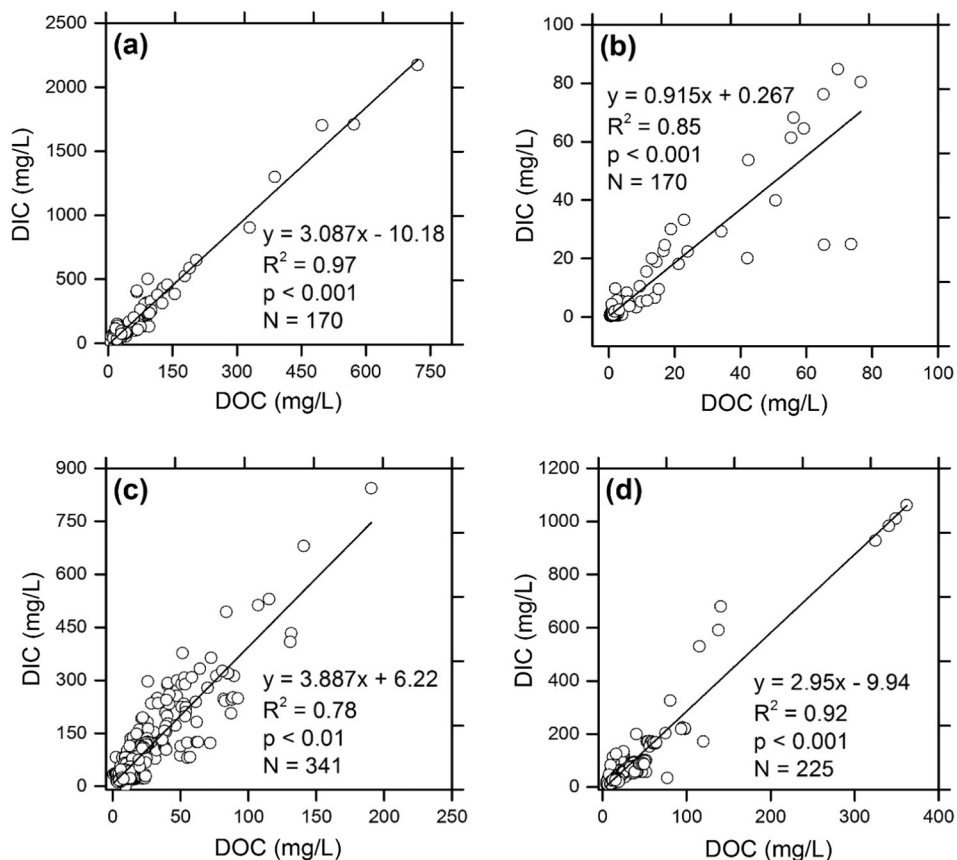


Fig. 5. Relationships between dissolved organic carbon (DOC) and dissolved inorganic carbon (DIC) concentrations for (a) underlying waters, (b) ice melted waters, (c) autumn water samples collected in 2011, 2014 and 2015, and (d) spring water samples collected in 2012, and 2015.

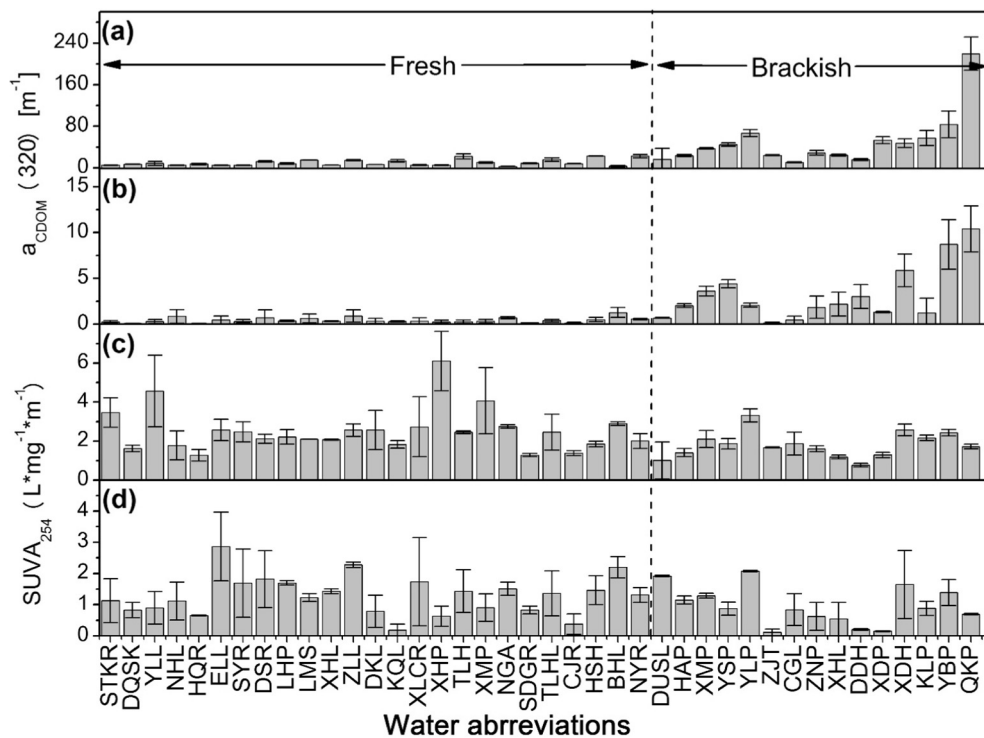


Fig. 6. Variation in CDOM absorption at 320 nm ( $a_{CDOM320}$ ) and specific UV absorption coefficient ( $SUVA_{254}$ ) in ice and underlying waters samples collected in lakes across the Songnen Plain in winter; (a)  $a_{CDOM320}$  for underlying waters and (b)  $a_{CDOM320}$  for melted lake ice from both freshwater and brackish lakes, (c)  $SUVA_{254}$  for underlying waters and (d)  $SUVA_{254}$  for melted lake ice. Full names of the study sites are listed in Table 1. Please note that the graphs are plotted on different scales.

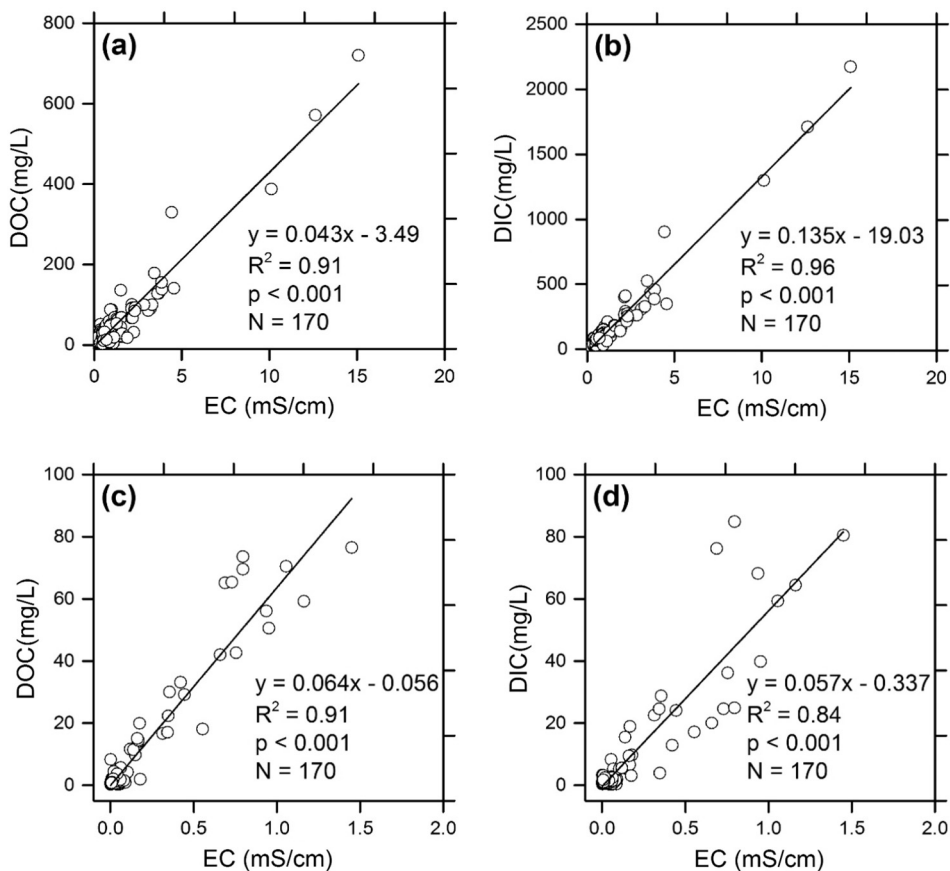


Fig. 7. Relationships between electric conductivity (EC) and dissolved carbon in lake waters across the Songnen Plain; (a) DOC and EC, (b) DIC and EC in underlying waters, (c) DOC and EC, (d) DIC and EC in melted lake ice samples.

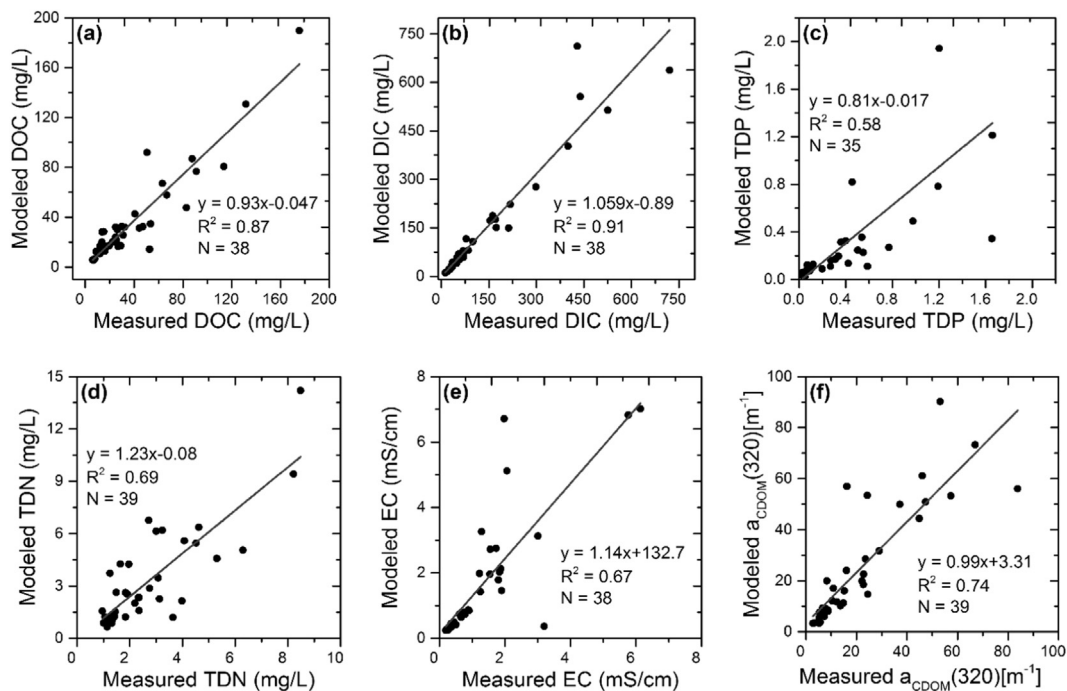


Fig. 8. Relationships between the calculated water chemical parameters in ice-covered lakes and the measured parameters in underlying waters, (a) DOC, (b) DIC, (c) TDP, (d) TDN, (e) EC and (f)  $a_{CDOM}(320)$ . Modeled values were derived from Eq. (3) using water depth, ice thickness and water chemical parameter values measured in water samples collected the previous autumn. Samples with extremely high values (deemed as outliers) were removed from Fig. 8, and please refer to Fig. S4 for the model performance with the whole data set.

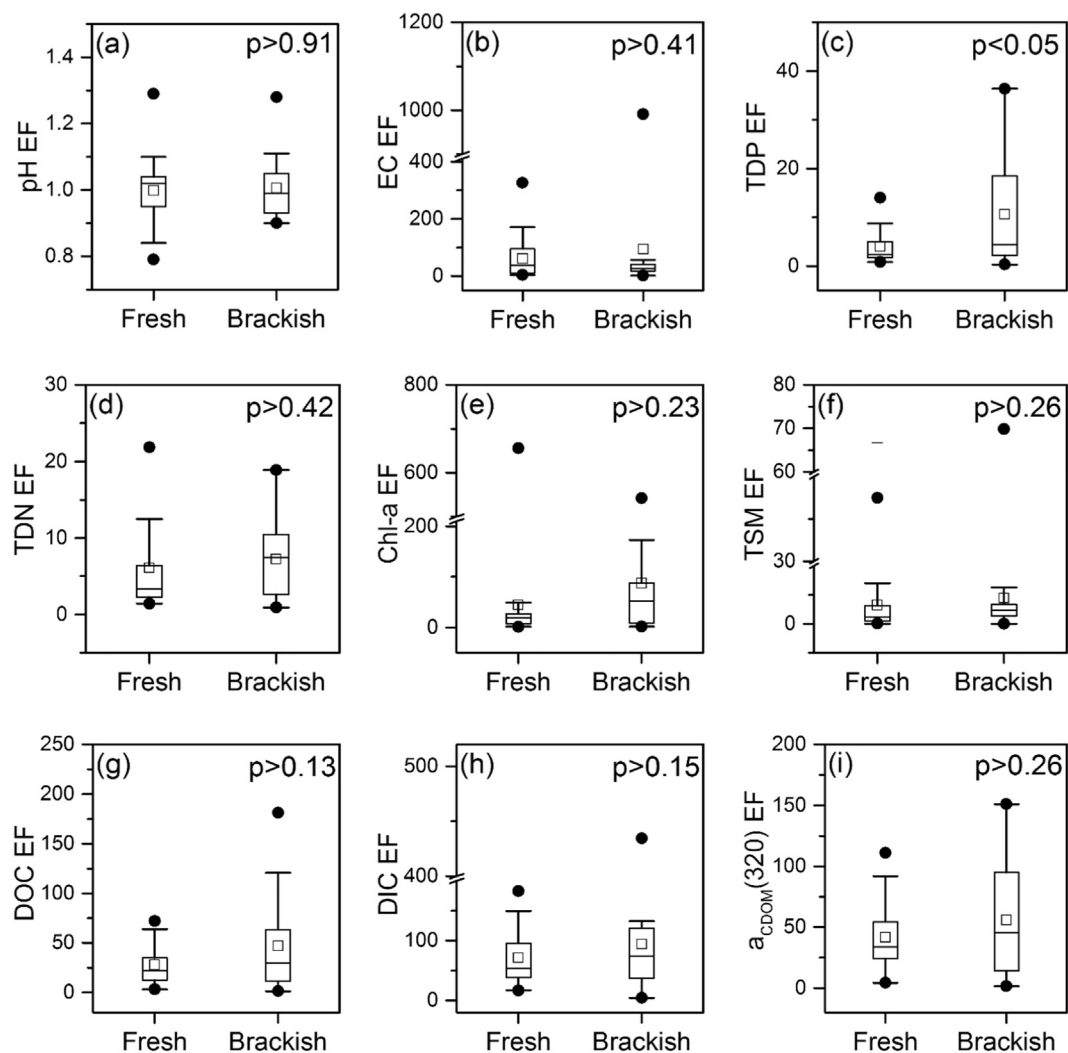


Fig. 9. Boxplots of exclusion factors (EF: water/ice) of various limnological parameters measured in freshwater lakes and brackish lakes across the Songnen Plain. In each box, the horizontal bar and the open square represent the median and mean, respectively. The edges of each box denote the 25th and 75th percentiles, the whiskers denote the 1st and 99th percentiles, and the filled circles represent outliers. Note that the differences in scale among the graphs.

bottom layer demonstrated an obvious variability, and a much higher variability was revealed for upper versus bottom than middle versus bottom layer.

## 4. Discussion

### 4.1. Limnological characteristics

Overall, most lakes in the Songnen Plain exhibited high EC and pH, a likely consequence of the climate and the hydro-geologic conditions of the region. Most of the brackish lakes are surrounded by saline soils (supplementary Fig. S1), and thus it is conceivable that surface runoff over these saline lands may have carried salt into these lakes. High levels of TDN and TDP were also measured in water samples from these lakes, which is strongly connected with non-point pollution from agricultural activities and other anthropogenic activities (Tong et al., 2017). The data presented here indicate that most of the aquatic systems selected for this study are nutrient-rich (TDN:  $3.6 \text{ mg N L}^{-1}$ ; TDP:  $0.56 \text{ mg P L}^{-1}$ ; Table 2). This nutrient enrichment may have contributed to algal proliferation in these water bodies, as suggested by the high concentration of Chl-a measured at most sites.

With the exception of pH, consistent and significant differences were found between melted lake ice and underlying waters with regard

to most of the water physical and chemical parameters (TDP, TDN, Chl-a, EC, TSM) considered in this study. Furthermore, the computed exclusion factors indicate strong exclusion of salts (EC), nutrients (TDP and TDN), and Chl-a from the ice phase and their presence in greater concentrations in the underlying waters (Table 3). These results are in line with the findings by Belzile et al. (2002) for several lakes in Canada, and solute exclusion effects are also supported by the work of Zhang et al. (2012), and Pieters and Lawrence (2009).

Interestingly, the exclusion factor for pH is close to unity, indicating that the acid-base status of lake waters was not significantly altered during ice formation, which is consistent with the findings of Zhang et al. (2012) from a study conducted at Ulansuhai Lake in Northern China. During the freezing process, changes of pH are related to the distribution of water ions between the liquid and ice phases, in which anions and cations are distributed between liquid and ice phases in different fashions. This partition imbalance is relaxed by the transfer of  $\text{H}^+$  and  $\text{OH}^-$  to each phase, resulting in the acidification of the liquid phase when the cation is better distributed in the ice phase than the anion, and in the basification in the opposite situation (Watanabe et al., 2014). In this study, the partition of the cations in these lakes may be preferential over anions during freezing process, which resulted in the acidification of sub-ice water. In other words, hydrogen ions are excluded from the ice matrix, this process should cause a slight pH

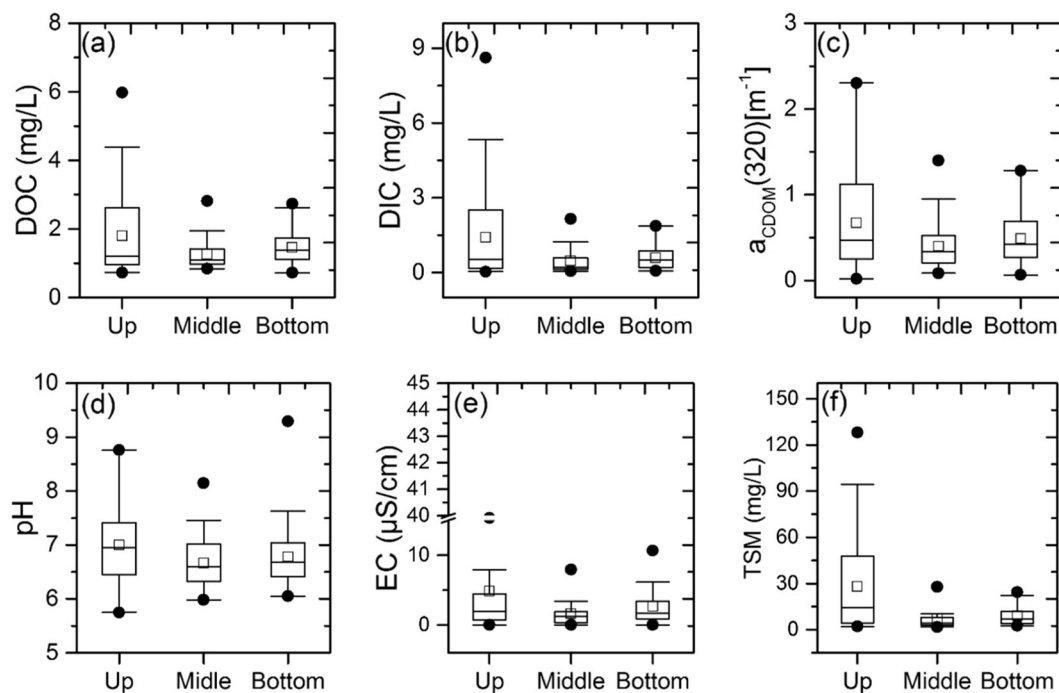


**Fig. 10.** Boxplots of various limnological parameters in the upper, middle and bottom layers of the ice cores collected in the Songnen Plain lakes in 2015. In each box, the horizontal bar and the open square represent the median and mean, respectively. The edges of each box denote the 25th and 75th percentiles, the whiskers denote the 1st and 99th percentiles, and the filled circles represent outliers.

increase in the ice layer and a pH decline in the sub-ice water. However, because of the buffer provided by the carbonate system (Weidner, 1979, Hare et al., 2013) and ion exchange processes (Gibbs, 1970, Saleem and Jeelani, 2017), our results showed that the pH in the sub-ice water was relatively stable.

It is important to note that, with the exception of TDP, no significant difference of EF was found between freshwater systems and brackish lakes (Fig. 9). The difference in TDP is an interesting observation, but difficult to explain using the data collected in the present study. Although the TSM concentration was generally lower in the overlying ice than that in the underlying water (Fig. 3f), the opposite was observed in some lakes (Table 3). A number of factors may have contributed to these variable results, e.g., resuspension of lake sediment just before freezing may have facilitated the incorporation of TSM into ice; on the other hand, ice prevents wind-driven turbulence in the underlying water and promotes sedimentation, which may have ultimately reduced TSM incorporated to ice. In the brackish lakes, we generally measured higher concentration of TDP in the underlying water than in the ice layer, but this observation was probably not related to the physical processes noted above (wind, erosion, resuspension). One can speculate, however, that redox conditions at the water-sediment interface may have played a role. In contrast to the freshwater systems, the brackish lakes are mainly closed-basin systems, without outlets and with long water residence time. Therefore, it is conceivable that anoxic conditions may periodically develop at the bottom of these lakes, thus promoting the release of sediment-bound P via reductive dissolution. This pool of released P may have contributed to the high TDP concentration measured in the underlying water at the brackish lakes. In fact, a moderate positive relationship ( $R^2 = 0.22$ ) was observed between pH and TDP in the brackish lakes, suggesting the consumption of protons ( $H^+$ ) during these reductive processes. It is unfortunate that ancillary water chemical parameters such as dissolved P and ORP (oxidation-reduction potential) were not measured during our sampling campaigns. These data would have allowed us to determine the validity of this interpretation.

The DOC concentrations (range: 2.2–720.3 mg CL<sup>-1</sup>; mean:

58.2 mg CL<sup>-1</sup>) measured in the ice-covered Songnen Plain lakes are some of the highest reported in the literature, including those reported by Sobek et al. (2007) from a survey of 7500 inland water bodies distributed over five continents (range: 0.1–332 mg CL<sup>-1</sup>; mean: 5.7 mg CL<sup>-1</sup>). Dissolved C concentrations in the Songnen Plain lakes exhibited significant temporal and spatial variations, likely reflecting seasonal changes in environmental conditions which, through their interactions with landscape attributes and hydrology, affect lake water volume, phytoplankton growth and C cycling in lake waters (Zhao et al., 2016). Spatially, concentrations of DOC and DIC were generally higher in the underlying water column than in the ice layer when the lakes were frozen in winter. This is mainly due to a redistribution of solutes during ice formation, with a preferential accumulation of DOC and DIC molecules in the aqueous phase underneath the frozen ice layer (Belzile et al., 2002; Xue et al., 2016), which was also demonstrated by a sea ice freezing experiment (Müller et al., 2013). A previous study has shown that dissolved solutes can be expelled from the solid ice matrix and transferred into the aqueous phase during the process of lake ice formation (Belzile et al., 2002; Zhang et al., 2012). This mechanism would be congruent with the high DOC and DIC exclusion factors measured in the present study (Table 3 and Fig. S4). The strength of this mechanism tends to increase in shallow water bodies similar to those found in the Songnen Plain (depth range: 1.4–8.4 m; mean: 2.8 m). Thus, these geomorphic features (shallow water depth, increase ice thickness) may facilitate the preferential distribution of solutes into the underlying waters during ice formation. These considerations are well encapsulated in our proposed model (Eq. (3)), and illustrated by the modeling results presented in Fig. 9a, b. As the denominator ( $D_w - I_i$ ) of Eq. (3) becomes smaller, the DOC enrichment of the underlying water is markedly enhanced. The averaged DOC exclusion factor was higher in the brackish lakes (48.3) than in the freshwater systems (28.2), suggesting that the mechanism described above is perhaps enhanced with increased DOC concentration in lake waters. The DOC exclusion factors measured in the present study were on average 9 times higher than reported by Belzile et al. (2002) for several Canadian lakes (range: 2.6–4.3; mean: 3.6). Some of the lakes are endorheic waters, high DOC

concentrations were prevailing in saline waters due to the evaporative condensed effect (Curtis and Adams, 1995; Song et al., 2013; Wen et al., 2016). The large difference in DOC concentration ( $58.2 \text{ mg CL}^{-1}$  in this study vs  $5.2 \text{ mg CL}^{-1}$  by Belzile et al., 2002) may have contributed to the difference in exclusion factors. Difference in water depth among the lakes investigated in the two studies could also be another contributing factor, where the lower water depth in the current study lakes further promotes the higher DOC concentration during ice formation. In addition, the good performance of the mass balanced model suggests that most of solutes were expelled to underlying waters during ice formation.

The spatial distribution of solutes within the ice layer (Fig. 10) may also be related to the ice growth rate and ice structure as determined by prevailing local weather conditions (Zhang et al., 2012). Spells of cold winter weather are common in Northeast China, and ice formation initiated during these weather events can proceed at an accelerated growth rate. Therefore, dissolved substances can migrate rapidly and become entrapped in the surface layer of a fast-growing ice sheet (Zhang et al., 2012). However, as the ice thickness increases, its growth rate would decline due to restriction on heat transfer from the underlying water to atmosphere, and that would result in less entrapment of substances into the growing ice layer (Belzile et al., 2002). Our results (Figs. 2 and 10) are consistent with such a mechanism, and are also congruent with the ice profiles described by Belzile et al. (2002) from their work at Char Lake, Canada. However, some lakes have shown different ice profiles, possibly due to differences in lake depth, types of ice (white versus clear) (Belzile et al., 2002; Salonen et al., 2010), and initial concentration of solutes before the initiation of ice formation. Further investigation is certainly needed to assess the significance of these parameters.

#### 4.2. Optical properties of CDOM

Compared to fresh waters, higher values for  $a_{\text{CDOM}(320)}$  were recorded in the brackish than in the freshwater lakes of the Songnen Plain, and the pattern holds for both melted ice and underlying waters, indicating that CDOM in the ice is mainly derived from the underlying waters. That would be different from sea ice in which a considerable amount of CDOM originates from algal biomass within the ice (Norman et al., 2011; Granskog et al., 2015). In the underlying waters, the  $\text{SUVA}_{254}$  values suggest that CDOM predominantly comprises high aromatic carbon fractions in freshwater lakes; whereas, in brackish waters, CDOM tends to predominantly include less aromaticity C fractions (Song et al., 2013, 2017). The same trend was observed for the melted lake ice water in both the freshwater and brackish lakes, and sea ice as well, further supporting our contention that CDOM in the ice layers originates from the underlying waters (Belzile et al., 2002; Müller et al., 2011, 2013; Xie et al., 2014). According to Belzile et al. (2002), CDOM contained in ice tends to include small size molecular and less aromatic organic substances. The aromaticity of CDOM retained in ice may change due to biological processes and photochemical degradation, especially with a prolonged exposure to solar irradiance (Müller et al., 2011; Kellerman et al., 2015; Xue et al., 2016). Previous studies indicated that photodegradation is the major driving force for CDOM absorption and component changes (Vähätalo & Wetzel, 2004; Zhang et al., 2010; Xue et al., 2016). These factors may contribute to the small molecular size and low aromaticity of CDOM present in the ice layer compared to the underlying waters (Müller et al., 2011). The presence of Chl-a in the ice layer suggests that autochthonous production of CDOM in ice was possible, but the potential impact of algal biomass on CDOM absorption characteristics is likely limited due to its low concentration as compared to CDOM originated from underlying parent waters. Additionally, the penetration of solar radiation through the ice layer can further induce photodegradation of CDOM into small molecular size organic components (Belzile et al., 2002; Müller et al., 2011; Xue et al., 2016). Taken together, all these factors may contribute

to the low molecular size and low aromaticity exhibited by CDOM contained in the overlying ice.

The geographical distribution of these two types of lakes encountered in the Songnen Plain could be an important factor explaining the differences between ice CDOM in freshwater and brackish lakes. The freshwater lakes are mostly located to the east, whereas the brackish waters occur predominantly on the western portion of the Songnen Plain where snow deposition is generally less (Table S2). Less snow coverage over the brackish lakes would facilitate a greater penetration of sunlight and thus a greater photo-degradation of CDOM contained in the ice sheet over these lakes (Belzile et al., 2001). Previous findings have proven that the CDOM in parent water is dominant factor regulating the CDOM optical property in ice (Müller et al., 2011, 2013; Xue et al., 2016). The differences in parent water CDOM absorption, and snow cover may partially explain the lower  $\text{SUVA}_{254}$  values for CDOM in ice over the brackish than over the freshwater lakes.

## 5. Conclusions

This study comprehensively investigated the concentrations and characteristics of dissolved carbon (DOC, DIC), CDOM, and other water parameters (TDP, TDN, Chl-a, EC, pH, and TSM) in lake ice and underlying waters in 40 lakes across the Songnen Plain, Northeast China. The lakes represent a range of hydrodynamic conditions (open flow versus closed systems without outlet) and salinity (freshwater vs. brackish waters). The study showed that, compared to the freshwater lakes, DOC and DIC concentrations tended to be elevated in the brackish lakes which predominantly occur in the endorheic region of the Songnen Plain. In winter, much higher concentrations of DOC, DIC, CDOM (as well as EC, TDP, TDN) were recorded in waters below the frozen lakes than in the ice layers. This stratification, numerically expressed as exclusion factor (water/ice ratio), was ascribed to a preferential redistribution of dissolved carbon and other solutes in the aqueous phase (instead in the ice matrix) during ice formation. This exclusion effect during ice formation could result in elevated concentration of solutes (e.g. TDP, TDN, EC) in the underlying waters, and that could have important water quality and ecological implications. In addition,  $a_{\text{CDOM}(320)}$  and  $\text{SUVA}_{254}$  indicate a predominance of C fractions with high molecular weight and aromaticity in the underlying waters compared to the overlying ice layer.

## Conflict of interest

The authors declare that there is no conflict of interest.

## Acknowledgments

The study was financially supported by the National Natural Science Foundation of China (Nos. 41730104 and 41471293) and the “Hundred Talents Program” of Chinese Academy of Sciences through a grant to Dr. Kaishan Song. The authors would also like to sincerely thank the students and staff from our research group for their assistance with samples collection and laboratory analysis. Finally, the authors are indebted to the anonymous reviewers and the handling editor for their very valuable comments and suggestions, enabling us to considerably improve the manuscript.

## Appendix A. Supplementary material

Supplementary data to this article can be found online at <https://doi.org/10.1016/j.jhydrol.2019.02.012>.

## References

Babin, M., Stramski, D., Ferrari, G.M., Claustre, H., Bricaud, A., Obolensky, G., Hoepffner,

- N., 2003. Variations in the light absorption coefficients of phytoplankton, nonalgal particles, and dissolved organic matter in coastal waters around Europe. *J. Geophys. Res.* 108 (C7), 3211.
- Belzile, C., Johannessen, S.C., Gosselin, M., Demers, S., Miller, W.L., 2000. Ultraviolet attenuation by dissolved and particulate constituents of first-year ice during late spring in an Arctic polynya. *Limnol. Oceanogr.* 45 (6), 1265–1273.
- Belzile, C., Vincent, W.F., Bibson, J.A.E., Hove, P.V., 2001. Bio-optical characteristics of the snow, ice, and water column of a perennially ice-covered lake in the High Arctic. *Can. J. Fish. Aquat. Sci.* 58, 2405–2418.
- Belzile, C., Gibson, J.A.E., Vincent, W.F., 2002. Colored dissolved organic matter and dissolved organic carbon exclusion from lake ice: implications for irradiance transmission and carbon cycling. *Limnol. Oceanogr.* 47 (5), 1283–1293.
- Brooks, P.D., Lemon, M.M., 2007. Spatial variability in dissolved organic matter and inorganic nitrogen concentration in a semiarid stream, San Pedro River, Arizona. *J. Geophys. Res.* 112, G03S05. <https://doi.org/10.1029/2006JG000262>.
- Carlson, R.E., 1977. A trophic state index for lakes. *Limnol. Oceanogr.* 22 (2), 361–369.
- Cole, J.J., Prairie, Y.T., Caraco, N.F., et al., 2007. Plumbing the global carbon cycle: Integrating inland waters into the terrestrial carbon budget. *Ecosystems* 10, 171–184.
- Curtis, P.J., Adams, H.E., 1995. Dissolved organic matter quantity and quality from freshwater and saltwater lakes in east-central Alberta. *Biogeochemistry* 30, 59–76.
- Duarte, C.M., Prairie, Y.T., Montes, C., Cole, J.J., Striegl, R., Melack, J., Downing, J.A., 2008. CO<sub>2</sub> emission from saline lakes: a global estimates of a surprisingly large flux. *J. Geophys. Res.* 113, G04041. <https://doi.org/10.1029/2007JG000637>.
- Gibbs, R.J., 1970. Mechanisms controlling world water chemistry. *Science* 170 (3962), 1088–1090.
- Granskog, M.A., Nomura, D., Müller, S., Krell, A., Toyota, T., Hattori, H., 2015. Evidence for significant protein-like dissolved organic matter accumulation in Sea of Okhotsk sea ice. *Ann. Glaciol.* 56 (69), 1–8.
- Gross, A., Boyd, C.E., 1998. A digestion procedure for the simultaneous determination of total nitrogen and total phosphorus in pond water. *J. World Aquacult. Soc.* 29 (3), 300–301.
- Hampton, S.E., Izmesteva, L., Moore, M.V., Katz, S.L., Dennis, B., Silow, E.A., 2008. Sixty years of environmental change in the world's largest freshwater lake—Lake Baikal, Siberia. *Global Change Biol.* 14, 1947–1958.
- Hampton, S.E., Galloway, A., Powers, S., Ozersky, T., Woo, K., et al., 2017. Ecology under lake ice. *Ecol. Lett.* 20 (1), 98–111.
- Hare, A.A., Wang, F., Barber, D., Geilfus, N.X., Galley, R.J., Rysgaard, S., 2013. pH evolution in sea ice grown at an outdoor experimental facility. *Mar. Chem.* 154, 46–54.
- Helms, J.R., Stubbins, A., Ritchie, J.D., Minor, E.C., Kieber, D.J., Mopper, K., 2008. Absorption spectral slopes and slope ratios as indicators of molecular weight, source, and photobleaching of chromophoric dissolved organic matter. *Limnol. Oceanogr.* 53, 955–969.
- Jaffé, R., McKnight, D., Maie, N., Cory, R., McDowell, W.H., Campbell, J.L., 2008. Spatial and temporal variations in DOM composition in ecosystems: the importance of long-term monitoring of optical properties. *J. Geophys. Res.* 113, G04032.
- Kellerman, A.M., Kothawala, D.N., Dittmar, T., Tranvik, L.J., 2015. Persistence of dissolved organic matter in lakes related to its molecular characteristics. *Nat. Geosci.* 8, 454–457.
- Lilbæk, G., Pomeroy, J.W., 2008. Ion enrichment of snowmelt runoff water caused by basal ice formation. *Hydrol. Process* 22, 2758–2766.
- Magnuson, J.J., et al., 2000. Historical trends in lake and river ice cover in the Northern Hemisphere. *Science* 289, 1743–1746.
- Mostofa, K.M.G., Wu, F.C., Yoshioka, T., Sakugawa, H., Tanoue, E., 2009. Dissolved organic matter in the aquatic environments. In: Wu, F.C., Xing, B. (Eds.), *Natural organic matter and its significance in the environment*. Science Press, Beijing, pp. 3–66.
- Mullen, P.C., Warren, S.G., 1988. Theory of the optical properties of lake ice. *J. Geophys. Res.* 93 (D7), 8403–8414.
- Müller, S., Vähätalo, A.V., Stedmon, C.A., Granskog, M.A., Norman, L., Aslam, S.N., Underwood, G., Dieckmann, G.S., Thomas, D.N., 2013. Selective incorporation of dissolved organic matter (DOM) during sea ice formation. *Mar. Chem.* 55, 148–157.
- Müller, S., Vähätalo, A., Granskog, M.A., Autio, R., Kaartokallio, H., 2011. Behaviors of dissolved organic matter during formation of natural and artificially grown Baltic Sea ice. *Ann. Glaciol.* 52 (57), 233–241.
- Mundy, C.J., Ehn, J.K., Barber, D.G., Michel, C., 2007. Influence of snow cover and algae on the spectral dependence of transmitted irradiance through Arctic landfast first-year sea ice. *J. Geophys. Res.* 112, C03007.
- Norman, L., Thomas, D.N., Stedmon, C.A., Granskog, M.A., Papadimitriou, S., Krapp, R.H., Meiners, K.M., Lannuzel, D., vanderMerwe, P., Dieckmann, G.S., 2011. The characteristics of dissolved organic matter (DOM) and chromophoric dissolved organic matter (CDOM) in Antarctic sea ice. *Deep-Sea Res. Pt II* 58, 1075–1091.
- Pacheco, F.S., Roland, F., Downing, J.A., 2013. Eutrophication reverses whole-lake carbon budgets. *Inland Waters* 4, 41–48.
- Pieters, R., Lawrence, G., 2009. Effect of salt exclusion from lake ice on seasonal circulation. *Limnol. & Oceanogr.* 54 (2), 401–412.
- Piiparinen, J., Enberg, S., Rintala, J.-M., Sommaruga, R., Majaneva, M., Autio, R., Vähätalo, A.V., 2015. The contribution of mycosporine-like amino acids, chromophoric dissolved organic matter and particles to the UV protection of sea-ice organisms in the Baltic Sea. *Photochem. Photobiol. Sci.* 14, 1025–1038.
- Pomeroy, J.W., Jones, H.G., Tranter, M., Lilbæk, G.R.O., 2005. Hydrochemical processes in snow-covered basins. *Encycl. Hydrol. Sci.* 1–14.
- Rysgaard, S., Glud, R.N., Sejr, M.K., Bendtsen, J., Christensen, P.B., 2007. Inorganic carbon transport during sea ice growth and decay: a carbon pump in polar seas. *J. Geophys. Res.* 112, C03016.
- Saleem, M., Jeelani, G., 2017. Geochemical, isotopic and hydrological mass balance approaches to constrain the lake water-groundwater interaction in Dal Lake, Kashmir Valley. *Environ. Earth Sci.* 76 (15), 533. <https://doi.org/10.1007/s12665-017-6865-5>.
- Salonen, K., Pulkkanen, M., Salmi, P., 2010. Humic fingers-water pockets migrating through lake ice. *Ver. Internat. Verein. Limnol.* 30 (10), 1664–1669.
- Spencer, R.G.M., Aiken, G.R., Wickland, K.P., Striegl, R.G., Hernes, P.J., 2008. Seasonal and spatial variability in dissolved organic matter quantity and composition from the Yukon River basin, Alaska. *Global Biogeochem. Cy.* 22, GB4002.
- Spencer, R.G.M., Butler, K.D., Aiken, G.R., 2012. Dissolved organic carbon and chromophoric dissolved organic matter properties of rivers in the USA. G03001. *J. Geophys. Res.* 117, 14 pp.
- Sobek, S., Tranvik, L.J., Prairie, Y.T., Kortelainen, P., Cole, J.J., 2007. Patterns and regulation of dissolved organic carbon: an analysis of 7,500 widely distributed lakes. *Limnol. Oceanogr.* 52, 1208–1219.
- Song, K.S., Zang, S.Y., Zhao, Y., Li, L., Du, J., Zhang, N.N., Wang, X.D., Shao, T.T., Liu, L., Guan, Y., 2013. Spatiotemporal characterization of dissolved Carbon for inland waters in semi-humid/semi-arid region, China. *Hydrol. Earth Syst. Sci.* 17, 4269–4281.
- Song, K.S., Zhao, Y., Wen, Z.D., Fang, C., Shang, Y.X., 2017. A systematic examination of the relationships between CDOM and DOC in inland waters in China. *Hydrol. Earth Syst. Sci.* 21, 5117–5141.
- Stedmon, C.A., Thams, D.N., Granskog, M., Kaartokallio, H., Papadimitriou, S., Kuosa, H., 2007. Characteristics of dissolved organic matter in baltic coastal sea ice: allochthonous or autochthonous origins? *Environ. Sci. Technol.* 41 (21), 7273–7279.
- Thomas, D.N., Kattner, G., Engbrodt, R., Giannelli, V., Kennedy, H., Haas, C., Dieckmann, G.S., 2001. Dissolved organic matter in Antarctic sea ice. *Ann. Glaciol.* 33, 297–303.
- Tong, Y.D., Zhang, W., Wang, X., Couture, R.M., Larssen, T., Zhao, Y., Li, J., Liang, H.J., Liu, X.Y., Bu, X., He, W., Zhang, Q., Lin, Y., 2017. Decline in Chinese lake phosphorus concentration accompanied by shift in sources since 2006. *Nat. Geosci.* 10, 507–511.
- Tranvik, L.J., Downing, J.A., Cotner, J.B., et al., 2009. Lakes and reservoirs as regulators of carbon cycling and climate. *Limnol. Oceanogr.* 54 (6), 2298–2314.
- Uusikivi, J., Vähätalo, A.V., Granskog, M.A., Sommaruga, R., 2010. Contribution of mycosporine-like amino acids and colored dissolved and particulate matter to sea ice optical properties and ultraviolet attenuation. *Limnol. Oceanogr.* 55 (2), 703–713.
- Vähätalo, A.V., Wetzel, R.G., 2004. Photochemical and microbial decomposition of chromophoric dissolved organic matter during long (months–years) exposures. *Mar. Chem.* 89, 313–326.
- Watanabe, H., Otsuka, T., Harada, M., Okada, T., 2014. Imbalance between anion and cation distribution at ice interface with liquid phase in frozen electrolyte as evaluated by fluorometric measurements of pH. *J. Phys. Chem. C* 118 (29), 15723–15731.
- Weishaar, J.L., Aiken, G.R., Bergamaschi, B.A., Fram, M.S., Fugii, R., Mopper, K., 2003. Evaluation of specific ultraviolet absorbance as an indicator of the chemical composition and reactivity of dissolved organic carbon. *Environ. Sci. Technol.* 37, 4702–4708.
- Weidner, B.V., 1979. pH of nature-waters. *Ohio J. Sci.* 79 52 52.
- Wen, Z.D., Song, K.S., Zhao, Y., Du, J., Ma, J.H., 2016. Influence of environmental factors on spectral characteristic of chromophoric dissolved organic matter (CDOM) in Inner Mongolia Plateau, China. *Hydrol. Earth Syst. Sci.* 20, 787–801.
- Wetzel, R.G., 2001. *Limnology: Lake and River Ecosystems*, third ed. Academic Press, New York.
- Weyhenmeyer, G., Kosten, S., Wallin, M., Tranvik, L., Jeppesen, E., et al., 2015. Significant fraction of CO<sub>2</sub> emissions from boreal lakes derived from hydrologic inorganic carbon inputs. *Nat. Geosci.* 8 (12), 933–936.
- Xie, H.X., Aubry, C., Zhang, Y., Song, G., 2014. Chromophoric dissolved organic matter (CDOM) in first-year sea ice in the western Canadian Arctic. *Mar. Chem.* 165, 25–35.
- Xue, S., Wang, C., Zhang, Z.H., Song, Y.T., Liu, Q., 2016. Photodegradation of dissolved organic matter in ice under solar irradiation. *Chemosphere* 144, 816–826.
- Zhang, Y.L., Zhang, E.L., Yin, Y., Van Dijk, M.A., Feng, L.Q., Shi, Z.Q., Liu, M.L., Qin, B.Q., 2010. Characteristics and sources of chromophoric dissolved organic matter in lakes of the Yungui Plateau, China, differing in trophic state and altitude. *Limnol. Oceanogr.* 55 (6), 2645–2659.
- Zhang, Y., Li, C.Y., Shi, X.H., Li, C., 2012. The migration of total dissolved solids during natural freezing process in Ulansuhai Lake. *J. Arid Land* 4 (1), 85–94.
- Zhao, Y., Song, K.S., Wen, Z.D., Li, L., Zang, S.Y., Shao, T.T., Li, S.J., Du, J., 2016. Seasonal characterization of CDOM for lakes in semiarid regions of Northeast China using excitation-emission matrix fluorescence and parallel factor analysis (EEM-PARAFAC). *Biogeosciences* 13, 1635–1645.
- Zhao, Y., Song, K.S., Shang, Y.X., Shao, T.T., Wen, Z.D., Lv, L.L., 2017. Characterization of CDOM of river waters in China using fluorescence excitation-emission matrix and regional integration techniques. *J. Geophys. Res.* 122 (8), 1940–1953.